

REDUCED BASIS APPROXIMATION AND A *POSTERIORI* ERROR ESTIMATES FOR PARAMETRIZED ELLIPTIC EIGENVALUE PROBLEMS *

IVAN FUMAGALLI¹, ANDREA MANZONI², NICOLA PAROLINI¹ AND MARCO VERANI¹

Abstract. We develop a new reduced basis (RB) method for the rapid and reliable approximation of parametrized elliptic eigenvalue problems. The method hinges upon dual weighted residual type *a posteriori* error indicators which estimate, for any value of the parameters, the error between the high-fidelity finite element approximation of the first eigenpair and the corresponding reduced basis approximation. The proposed error estimators are exploited not only to certify the RB approximation with respect to the high-fidelity one, but also to set up a greedy algorithm for the offline construction of a reduced basis space. Several numerical experiments show the overall validity of the proposed RB approach.

Mathematics Subject Classification. 65M15, 65N25, 65N30, 78M34.

Received April 20, 2015. Revised January 20, 2016. Accepted January 22, 2016.

1. INTRODUCTION

The efficient solution of parametrized eigenproblems represents a key numerical challenge in several contexts of applied interest. Acoustics, optics and structural mechanics are just three broad fields where eigenproblems are ubiquitous. In several cases, we might be interested to solve this kind of problems in a range of different settings or scenarios, each one characterized by different material properties or physical coefficients, source terms and/or their localization, geometrical configurations. This occurs very often in sensitivity analyses, input/output (or system response) evaluations, as well as in optimization contexts, such as optimal control and optimal design problems. Concerning these latter class, some relevant examples are (i) the control of structural vibrations or (ii) the design of optical devices. In the former case, the resonant frequencies of a vibrating system might be pushed away from a specified window by changing the geometry of the structure, or adding mass to it [30]. In the latter case, the optimal localization of eigenfunctions in an inhomogeneous medium arises in the design of photonic bandgap structures, which are the optical analogues of electronic semiconductors. By introducing patterned defects into a photonic bandgap structure, it is possible to control the propagation of light within the structure [11]. A further relevant application which requires the efficient solution of eigenproblems is population

Keywords and phrases. Parametrized eigenvalue problems, reduced basis method, *a posteriori* error estimation, greedy algorithm, dual weighted residual.

* Marco Verani has been partially supported by GNCS-INDAM and by the Italian research grant Prin 2012 2012HBLYE4 “Metodologie innovative nella modellistica differenziale numerica”.

¹ MOX – Modellistica e Calcolo Scientifico, Dipartimento di Matematica “F. Brioschi”, Politecnico di Milano, via Bonardi 9, 20133 Milano, Italy. ivan.fumagalli@polimi.it; nicola.parolini@polimi.it; marco.verani@polimi.it

² CMCS-MATHICSE-SB, Ecole Polytechnique Fédérale de Lausanne, Station 8, 1015 Lausanne, Switzerland.
andrea.manzoni@epfl.ch

dynamics, where one may be interested in, *e.g.*, determining the optimal spatial arrangement of favorable and unfavorable regions for a species to survive [17].

Motivated by these (and many other) examples, we develop in this work a numerical technique for the efficient solution of parametrized elliptic eigenproblems, relying on the so-called *reduced basis* (RB) method. RB methods enable to solve parametrized partial differential equations (PDEs) in a very short amount of time – possibly, in a real-time way – by involving very few degrees of freedom, if compared to usual high-fidelity approximation techniques, such as the Finite Element (FE) or the Finite Volume (FV) method.

The RB method seeks the solution of a PDE problem within a low-dimensional, problem-dependent approximation space, whose basis is given by suitably chosen snapshots of the high-fidelity problem, that is, by PDE solutions computed for selected parameter values. A greedy algorithm relying on a residual-based *a posteriori* error estimate is usually exploited to sample the parameter space efficiently, in order to build reduced spaces of very low dimension. This is a widely used technique in the RB approximation of parametrized elliptic and parabolic PDEs, featuring a very efficient offline/online computational procedure. Algebraic structures related to reduced operators, as well as the reduced basis functions, can be computed during the *offline* phase, so that the online evaluation of the reduced problem, for any new parameter value, can be performed in a very inexpensive way. See *e.g.* [34] for several discussions and details.

Despite RB methods have been applied to a huge variety of problems [29] in the last decade – including heat and mass transfer [15], fluid flows modelled by Stokes [36] and Navier–Stokes [20, 23] equations, electromagnetism [13], optimal control problems [9, 28], optimal design problems [19, 24] – the evaluation of efficient RB approximations of parametrized eigenproblems has not been deeply analyzed. In their pioneering work [21], Rovas, Maday and Patera propose a RB method for the rapid and reliable approximation of the smallest eigenvalue in the context of parametrized symmetric elliptic eigenvalue problems. They also develop a first *a posteriori* error estimate (see also [22]), which provides however a bound just on the eigenvalue and not on the corresponding eigenfunction, and is employed only in the *online* phase to certify the RB approximation. Moreover, they consider a RB space made of the first two eigenfunctions evaluated for a selected set of parameter values, without taking advantage of any greedy adaptive procedure, to characterize the smallest eigenpair. Hence, the *a posteriori* error bound is not employed for the sake of an efficient exploration of the parameter space during the offline construction of the reduced basis. Further related developments can be found *e.g.* in [32, 35]. More recently, a growing interest has been oriented to computational reduction for large-scale eigenvalue problems: (i) the first example of construction of RB spaces through a greedy method exploiting asymptotic *a posteriori* error bounds was provided by Pau [31] for multiple eigenvalues in few specific test cases arising in electronic structure calculations; (ii) a component-based approach has been introduced for fast evaluation of parameter-dependent eigenproblems, in the context of the so-called static condensation RB method [18], where *a posteriori* error estimators are provided for eigenvalues only; (iii) greedy procedures for high-dimensional (non-parametrized) eigenvalue problems in the context of the so-called proper generalized decomposition methods [1] have been explored in [7], without considering *a posteriori* error analysis. An *a posteriori* error bound for multiple eigenvalues (but not eigenvectors) has been recently proposed in [10], however considering eigenproblems with only affine parametric dependence. As a matter of fact, developing sharp, reliable and inexpensive *a posteriori* error estimates for eigenpairs seems to be a critical aspect, which makes the RB approximation of parametrized eigenproblems a challenging task.

The goal of this paper is to develop a new RB method for the rapid and effective approximation of parametrized elliptic eigenvalue problems. The method hinges upon the use of reliable and computable dual weighted residual (DWR) type error estimators. Indeed, in the same spirit of the work by Heuveline and Rannacher [16] (see also [4]), we provide *a posteriori* estimates for the error between the high-fidelity (FE) smallest eigenpair $(\lambda_h(\boldsymbol{\mu}), u_h(\boldsymbol{\mu}))$ and the corresponding RB approximation $(\lambda_N(\boldsymbol{\mu}), u_N(\boldsymbol{\mu}))$, for any parameter value $\boldsymbol{\mu} \in \mathcal{D} \subset \mathbb{R}^P$. Moreover, the reliability of the error estimates is proved. We take advantage of this result not only to certify the RB approximation with respect to the high-fidelity one, but also to set a greedy algorithm for the efficient construction of a low-dimensional reduced basis space. In particular, we develop an offline/online strategy to deal with both the assembling of the reduced algebraic structures and the evaluation

of (dual norms of) residuals in a very efficient way. The efficacy of the whole computational framework is assessed through several numerical test cases, where the final goal is the localization of eigenfunctions in a domain representing a medium with $\boldsymbol{\mu}$ -dependent physical properties. To this aim, we consider both affinely and non-affinely parametrized eigenproblems; concerning the latter, the empirical interpolation method [2] is used to recover an (approximate) affine parametric expression for the sake of computational efficiency of the RB method.

The structure of the paper is as follows. In Section 2 we introduce the parametrized elliptic eigenvalue problem together with its high-fidelity FE approximation. In Section 3 we introduce the reduced basis approximation and a greedy algorithm for the efficient assembling of reduced basis spaces. In Section 4, relying on the dual weighted residual theory, we introduce our *a posteriori* error estimates for the parametrized eigenvalue problem and prove their reliability. We also discuss the efficient evaluation of some problem-dependent quantities appearing in our error estimates. Finally, in Section 5 several numerical results, related to both affinely and non-affinely parametrized eigenproblems, assess the computational efficacy of our RB approach.

2. PARAMETRIZED ELLIPTIC EIGENVALUE PROBLEMS

Our goal is to provide a very fast and reliable numerical approximation for the following generalized eigenvalue problem: given $\boldsymbol{\mu} \in \mathcal{D} \subseteq \mathbb{R}^P$, being \mathcal{D} a given parameter space, find a pair $(\lambda, u) = (\lambda(\boldsymbol{\mu}), u(\boldsymbol{\mu}))$ such that

$$\begin{cases} -\Delta u = \lambda \varepsilon(\boldsymbol{\mu}) u & \text{in } \Omega \subset \mathbb{R}^2, \\ u = 0 & \text{on } \partial\Omega, \end{cases} \tag{2.1}$$

subject to the normalization constraint

$$\int_{\Omega} \varepsilon(\boldsymbol{\mu}) u^2 \, d\mathbf{x} = 1, \tag{2.2}$$

where $\Omega \subset \mathbb{R}^2$ is a Lipschitz domain and, for any $\boldsymbol{\mu} \in \mathcal{D}$, $\varepsilon(\boldsymbol{\mu}) \in L^\infty(\Omega)$ is a strictly positive function. Moreover, we assume that there exist $\varepsilon_0, \varepsilon_\infty \in \mathbb{R}_+$ such that $0 < \varepsilon_0 \leq \varepsilon(\mathbf{x}; \boldsymbol{\mu}) \leq \varepsilon_\infty$ for a.e. $\mathbf{x} \in \Omega$ and all $\boldsymbol{\mu} \in \mathcal{D}$. In particular, denoting by $\{\lambda^{(n)}(\boldsymbol{\mu})\}_{n \in \mathbb{N}}$ the sequence of the eigenvalues of problem (2.1) sorted in ascending order, we are interested in determining the smallest eigenvalue $\lambda^{(1)}(\boldsymbol{\mu})$ and the corresponding eigenfunction $u^{(1)}(\boldsymbol{\mu})$, for any $\boldsymbol{\mu} \in \mathcal{D}$. After presenting the properties of the continuous problem (2.1), in this section we introduce and analyze its high-fidelity discretization based on the Galerkin-FE method. Instead of the Laplacian operator (here considered for the sake of simplicity), the more general case of an elliptic, second-order operator $-\nabla \cdot (K(\mathbf{x})\nabla)$ could be addressed as well, being $K = K(\mathbf{x})$ a $\boldsymbol{\mu}$ -independent, symmetric and uniformly positive definite matrix for any $\mathbf{x} \in \Omega$.

2.1. Parametrized formulation and high-fidelity approximation

From the theory of symmetric elliptic operators (see, e.g., [12]), problem (2.1) is well posed, all its eigenvalues are strictly positive, and the multiplicity of $\lambda^{(1)}$ is one, so that the eigenpair $(\lambda^{(1)}(\boldsymbol{\mu}), u^{(1)}(\boldsymbol{\mu}))$ is uniquely determined, for each $\boldsymbol{\mu} \in \mathcal{D}$. Let us introduce the space $V = H_0^1(\Omega)$ and the bilinear forms $a(\cdot, \cdot) : V \times V \rightarrow \mathbb{R}$ and $b(\cdot, \cdot; \boldsymbol{\mu}) : V \times V \times \mathcal{D} \rightarrow \mathbb{R}$ defined by

$$a(\psi_1, \psi_2) = (\nabla\psi_1, \nabla\psi_2), \quad b(\psi_1, \psi_2; \boldsymbol{\mu}) = (\varepsilon(\boldsymbol{\mu})\psi_1, \psi_2) \quad \forall \psi_1, \psi_2 \in V, \forall \boldsymbol{\mu} \in \mathcal{D}.$$

In these definitions, and throughout the whole paper, we denote by (\cdot, \cdot) and $\|\cdot\|$ the $L^2(\Omega)$ inner product and the induced norm, respectively. Moreover, for any $\varphi \in L^2(\Omega)$, we also define the norm $\|\varphi\|_b = \sqrt{b(\varphi, \varphi)}$, which is equivalent to the L^2 norm $\|\cdot\|$, since

$$\sqrt{\varepsilon_0}\|\psi\| \leq \|\psi\|_b \leq \sqrt{\varepsilon_\infty}\|\psi\|. \tag{2.3}$$

The weak formulation of problem (2.1) reads as follows: given $\boldsymbol{\mu} \in \mathcal{D}$, find $\lambda = \lambda(\boldsymbol{\mu}) \in \mathbb{R}$ and $u = u(\boldsymbol{\mu}) \in V$ such that

$$\begin{aligned} a(u, \psi) &= \lambda b(u, \psi; \boldsymbol{\mu}) \quad \forall \psi \in V, \\ b(u, u; \boldsymbol{\mu}) &= 1. \end{aligned} \tag{2.4}$$

It is worth recalling that the first eigenvalue of a problem of the form (2.4) minimizes its Rayleigh quotient, *i.e.*

$$\lambda^{(1)}(\boldsymbol{\mu}) = \min_{\psi \in V} \frac{a(\psi, \psi)}{b(\psi, \psi; \boldsymbol{\mu})}, \tag{2.5}$$

and that the other eigenvalues are such that

$$\lambda^{(n)}(\boldsymbol{\mu}) = \min_{\psi \in V^{(n)}} \frac{a(\psi, \psi)}{b(\psi, \psi; \boldsymbol{\mu})}. \tag{2.6}$$

that is, they satisfy property (2.5) on the lower-dimensional subspaces

$$V^{(n)} = \left(\text{span}\{u^{(1)}, \dots, u^{(n-1)}\} \right)^{\perp_b},$$

where the orthogonality has to be meant with respect to the bilinear form b .

Since for the applications presented in Section 5 the $\boldsymbol{\mu}$ -dependency only affects the function $\varepsilon(\boldsymbol{\mu})$, the framework addressed in this paper does not include a bilinear form $a(\cdot, \cdot)$ that is $\boldsymbol{\mu}$ -dependent, too. Nevertheless, the analysis carried out to derive *a posteriori* error bounds, as well as the construction of RB spaces, can be extended with no additional efforts to the more general case of $\boldsymbol{\mu}$ -dependent bilinear forms $a(\cdot, \cdot, \boldsymbol{\mu})$ – concerning instead computational efficiency, this case could entail additional costs, see *e.g.* Remark 4.9.

Remark 2.1. From now on, when no misunderstanding occurs, the principal eigenpair $(\lambda^{(1)}, u^{(1)})$ will be denoted by (λ, u) .

2.2. High-fidelity approximation of the problem

Let us now introduce the high-fidelity approximation of the eigenproblem (2.4) by considering a Galerkin-FE approximation. To this end, let us introduce a FE subspace $V_h \subset V$ of dimension $\dim(V_h) = N_h$ where $V_h = H_0^1(\Omega) \cap X_h^r(\Omega)$ and

$$X_h^r(\Omega) = \{\psi_h \in C^0(\overline{\Omega}) : \psi_h|_K \in \mathbb{P}_r(K) \ \forall K \in \mathcal{T}_h\}.$$

Here we denote by \mathcal{T}_h a conforming and regular triangulation of the domain Ω and by $\mathbb{P}_r(K)$ the set of polynomials on $K \in \mathcal{T}_h$ with degree not greater than r . The high-fidelity approximation of problem (2.4) reads as follows: given $\boldsymbol{\mu} \in \mathcal{D}$, find $u_h = u_h(\boldsymbol{\mu}) \in V_h$ and $\lambda_h = \lambda_h(\boldsymbol{\mu}) \in \mathbb{R}$ such that

$$\begin{aligned} a(u_h, \psi_h) &= \lambda_h b(u_h, \psi_h; \boldsymbol{\mu}) \quad \forall \psi_h \in V_h, \\ b(u_h, u_h; \boldsymbol{\mu}) &= 1. \end{aligned} \tag{2.7}$$

Denoting by $\{\lambda_h^{(n)}\}_{n \in \mathbb{N}}$ the sequence of the eigenvalues of problem (2.7), sorted in ascending order, we are interested to compute $\lambda_h = \lambda_h^{(1)}$ and the corresponding eigenfunction $u_h = u_h^{(1)}$. In particular, we assume that the partition \mathcal{T}_h is sufficiently fine so that λ_h is simple like its continuous counterpart λ . Moreover, let us denote by $\{\varphi_i\}_{i=1}^{N_h}$ a basis of V_h ; the algebraic formulation of problem (2.7) reads as follows:

$$\begin{aligned} A\mathbf{U}_h &= \lambda_h B(\boldsymbol{\mu})\mathbf{U}_h, \\ \mathbf{U}_h^T B(\boldsymbol{\mu})\mathbf{U}_h &= 1, \end{aligned} \tag{2.8}$$

where

$$A_{ij} = a(\varphi_j, \varphi_i), \quad B_{ij}(\boldsymbol{\mu}) = b(\varphi_j, \varphi_i; \boldsymbol{\mu}), \quad i, j = 1, \dots, N_h$$

and $\mathbf{U}_h = \mathbf{U}_h(\boldsymbol{\mu})$ is the vector of the degrees of freedom of $u_h(\boldsymbol{\mu})$, that is, we can express $u_h = \sum_{i=1}^{N_h} (\mathbf{U}_h)_i \varphi_i$. Moreover, let us denote by M the L^2 mass matrix, whose elements are given by

$$M_{ij} = (\varphi_j, \varphi_i), \quad i, j = 1, \dots, N_h.$$

We point out that solving problem (2.8) might entail severe computational costs, since A and $B(\boldsymbol{\mu})$ are $N_h \times N_h$ matrices, where the dimension N_h can be very larger. Moreover, since B depends on the parameter $\boldsymbol{\mu}$, its assembling is in principle required for any new value of $\boldsymbol{\mu} \in \mathcal{D}$. In Section 3 we will come back on both these issues.

To conclude this section, we provide bounds for the discrete eigenvalue λ_h . Since $V_h \subset V = H_0^1(\Omega)$, it is easy to check that, for any $\boldsymbol{\mu} \in \mathcal{D}$,

$$\lambda_h(\boldsymbol{\mu}) = \inf_{\psi_h \in V_h} \frac{a(\psi_h, \psi_h)}{b(\psi_h, \psi_h; \boldsymbol{\mu})} \geq \inf_{\psi \in V} \frac{a(\psi, \psi)}{b(\psi, \psi; \boldsymbol{\mu})} = \lambda(\boldsymbol{\mu}). \quad (2.9)$$

Thus, the discrete eigenvalue λ_h is always an upper bound for the continuous eigenvalue λ . Moreover, we have that

$$\lambda \leq \lambda_h \leq \frac{\chi_h}{\varepsilon_0} \quad (2.10)$$

by recalling that $b(\psi_h, \psi_h; \boldsymbol{\mu}) \geq \varepsilon_0(\psi_h, \psi_h)$ for any $\boldsymbol{\mu}$ and denoting by χ_h the principal eigenvalue of the following problem:

$$(\nabla z_h, \nabla \psi_h) = \chi_h(z_h, \psi_h) \quad \forall \psi_h \in V_h. \quad (2.11)$$

Remark 2.2. We point out that χ_h is related to the discrete Poincaré constant $c_{\Omega, h}$ fulfilling the following inequality:

$$\|\psi_h\| \leq c_{\Omega, h} \|\nabla \psi_h\| \quad \forall \psi_h \in V_h. \quad (2.12)$$

Indeed, exploiting the formulation of problem (2.11) in terms of Rayleigh quotient, we obtain that $\chi_h = 1/c_{\Omega, h}^2$; hence, the bounds (2.10) can be rewritten as

$$\lambda \leq \lambda_h \leq \frac{1}{\varepsilon_0 c_{\Omega, h}^2}. \quad (2.13)$$

2.3. Affine expansion and empirical interpolation

For the sake of computational efficiency of the RB method, we require a further assumption on the parametrized bilinear form $b(\cdot, \cdot; \boldsymbol{\mu})$. In fact, a generic dependence of the weight function ε on the parameter $\boldsymbol{\mu}$ has been considered so far. A very favorable case is the one where the parametric dependence of the problem coefficients is affine; in our case, this means that we can express

$$\varepsilon(\mathbf{x}; \boldsymbol{\mu}) = \sum_{k=1}^Q \Theta_k(\boldsymbol{\mu}) \varepsilon_k(\mathbf{x}) \quad (2.14)$$

so that, consequently,

$$b(\cdot, \cdot; \boldsymbol{\mu}) = \sum_{k=1}^Q \Theta_k(\boldsymbol{\mu}) b_k(\cdot, \cdot) = \sum_{k=1}^Q \Theta_k(\boldsymbol{\mu}) (\varepsilon_k(\mathbf{x}) \cdot, \cdot). \quad (2.15)$$

An affine parametric dependence like (2.15) is a key property to be fulfilled in order to reduce the computational effort entailed by the assembling of $\boldsymbol{\mu}$ -dependent operators. In fact, the $\boldsymbol{\mu}$ -independent forms $b_k(\cdot, \cdot)$ can

be assembled once for all, then evaluating the form $b(\cdot, \cdot; \boldsymbol{\mu})$ for different values of $\boldsymbol{\mu}$ just requires the evaluation of the scalar functions $\Theta_k(\boldsymbol{\mu})$, $k = 1, \dots, Q$.

In general, the dependence of the weight function ε on $\boldsymbol{\mu}$ can be nonlinear, so that finding an expression under the form (2.14) is not straightforward. To address this kind of problems, the so-called *empirical interpolation method* (EIM) has been introduced in [2], and subsequently used in several applications of the RB method (see, e.g., [24, 34] for further details). Such a technique enables to recover (at least in an approximate way) an affine expression of $\boldsymbol{\mu}$ -dependent functions operators; in our case, we end up with

$$\varepsilon(\mathbf{x}; \boldsymbol{\mu}) = \tilde{\varepsilon}(\mathbf{x}; \boldsymbol{\mu}) + \delta(\mathbf{x}; \boldsymbol{\mu}) = \sum_{k=1}^Q \Theta_k(\boldsymbol{\mu}) \varepsilon_k(\mathbf{x}) + \delta(\mathbf{x}; \boldsymbol{\mu}) \tag{2.16}$$

where $\tilde{\varepsilon}$ denotes the EIM approximation of ε and $\|\delta(\cdot; \boldsymbol{\mu})\|_{L^\infty(\Omega)} \leq \varepsilon_{\text{tol}}^{EIM}$, for any $\boldsymbol{\mu} \in \mathcal{D}$, with $\varepsilon_{\text{tol}}^{EIM}$ a small, prescribed tolerance.

We will consider both affine and non-affine eigenproblems, that is, cases where the affine dependence property (2.14) (i) is automatically satisfied, or (ii) is not *built-in* in the definition of $\varepsilon(\mathbf{x}; \boldsymbol{\mu})$ and, therefore, has to be recovered by applying EIM. In this latter case, We can easily characterize the effect of the EIM approximation in terms of the approximation error on the high-fidelity FE eigenvalues. Let us consider two instances of problem (2.7), one with the weight function ε and one with its EIM approximation $\tilde{\varepsilon}$. Correspondingly, let us denote by $\tilde{B}(\boldsymbol{\mu}) \in \mathbb{R}^{N_h \times N_h}$ the matrix obtained by replacing $\varepsilon(\mathbf{x}, \boldsymbol{\mu})$ with $\tilde{\varepsilon}(\mathbf{x}; \boldsymbol{\mu})$. Moreover, let us denote by $\lambda_h^{(k)}$ and $\tilde{\lambda}_h^{(k)}$ the k -th eigenvalue of the two corresponding problems, respectively. Thanks to the extension of the Bauer–Fike theorem [14] to generalized eigenproblems (see Appendix A), it is straightforward to show that for the first eigenvalue $\lambda_h^{(1)}(\boldsymbol{\mu})$ the following relation holds:

$$\begin{aligned} \min_k \frac{|\tilde{\lambda}_h^{(k)}(\boldsymbol{\mu}) - \lambda_h^{(1)}(\boldsymbol{\mu})|}{\lambda_h^{(1)}(\boldsymbol{\mu})} &\leq \|\tilde{\varepsilon}(\cdot; \boldsymbol{\mu}) - \varepsilon(\cdot; \boldsymbol{\mu})\|_{L^\infty(\Omega)} \|B^{-1/2}\|_2 \|M\|_2 \|B^{-1/2}\|_2 \\ &\leq \frac{1}{\varepsilon_0} \|\tilde{\varepsilon}(\cdot; \boldsymbol{\mu}) - \varepsilon(\cdot; \boldsymbol{\mu})\|_{L^\infty(\Omega)} \kappa_2(M), \quad \forall \boldsymbol{\mu} \in \mathcal{D}, \end{aligned} \tag{2.17}$$

where $\|\cdot\|_2$ denotes the matrix Euclidean norm, and $\kappa_2(M)$ is the condition number of the mass matrix M ³. Therefore, by imposing a sufficiently small tolerance $\varepsilon_{\text{tol}}^{EIM}$ on the EIM approximation of ε , we can easily control the influence of such approximation on the error in the computed eigenvalues⁴.

3. THE REDUCED BASIS APPROXIMATION

The RB method builds up the solution of a parametrized PDE as a Galerkin solution of a reduced problem, obtained by projecting the original problem onto a low dimensional subspace, whose basis functions are obtained from the snapshot solutions, *i.e.* the solutions of the high-fidelity PDE problem, evaluated for a suitably chosen set of parameter values.

Let us consider the first eigenfunction $u_h(\boldsymbol{\mu}^{(i)})$, $i = 1, \dots, N$, obtained by solving problem (2.7) for $N \ll N_h$ different parameter values $\boldsymbol{\mu}^{(i)}$, and introduce the linear space

$$V_N = \text{span}\{u_h(\boldsymbol{\mu}^{(1)}), \dots, u_h(\boldsymbol{\mu}^{(N)})\} \subset V_h.$$

³This particular result holds using the Euclidean matrix norm, because in this norm

$$\|B^{-1/2}\|_2 = \max_{\sigma \in \lambda(B^{-1/2})} |\sigma| = \sqrt{\max_{\rho \in \lambda(B^{-1})} |\rho|} = \sqrt{\|B^{-1}\|_2} \leq \sqrt{\frac{1}{\varepsilon_0} \|M^{-1}\|_2}, \tag{2.18}$$

where $\lambda(B^{-1/2})$ and $\lambda(B^{-1})$ denote the spectra of $B^{-1/2}$ and B^{-1} , respectively.

⁴For the mesh of about 8500 elements used in the numerical tests of this paper, $\kappa_2(M) \simeq 24.5$.

The RB approximation is obtained by projecting problem (2.4) onto the space V_N and thus it reads as follows: given $\boldsymbol{\mu} \in \mathcal{D}$, find $u_N = u_N(\boldsymbol{\mu}) \in V_N$ and $\lambda_N = \lambda_N(\boldsymbol{\mu}) \in \mathbb{R}$ such that

$$\begin{aligned} a(u_N, \psi_N) &= \lambda_N b(u_N, \psi_N; \boldsymbol{\mu}) \quad \forall \psi_N \in V_N, \\ b(u_N, u_N; \boldsymbol{\mu}) &= 1. \end{aligned} \quad (3.1)$$

Remark 3.1. In what follows, we assume that also for problem (3.1) the first eigenvalue $\lambda_N(\boldsymbol{\mu}) = \lambda_N^{(1)}(\boldsymbol{\mu})$ is simple. A sufficient condition to ensure this property is, for instance, that $\lambda_N(\boldsymbol{\mu})$ and the second eigenvalue $\lambda_N^{(2)}(\boldsymbol{\mu})$ converge to their FE counterparts, namely $\lambda_N(\boldsymbol{\mu}) \rightarrow \lambda_h(\boldsymbol{\mu})$, $\lambda_N^{(2)}(\boldsymbol{\mu}) \rightarrow \lambda_h^{(2)}(\boldsymbol{\mu})$ for $N \rightarrow N_h$, for any $\boldsymbol{\mu} \in \mathcal{D}$.

Remark 3.2. Since V_N is a subspace of V_h , it is easy to see that, for any $\boldsymbol{\mu} \in \mathcal{D}$,

$$\lambda_N(\boldsymbol{\mu}) = \inf_{\psi_N \in V_N} \frac{a(\psi_N, \psi_N)}{b(\psi_N, \psi_N; \boldsymbol{\mu})} \geq \inf_{\psi_h \in V_h} \frac{a(\psi_h, \psi_h)}{b(\psi_h, \psi_h; \boldsymbol{\mu})} = \lambda_h(\boldsymbol{\mu}). \quad (3.2)$$

Thus, the RB eigenvalue λ_N is always an upper bound for the high-fidelity eigenvalue λ_h , and together with (2.9), we end up with the following relation,

$$\lambda_N(\boldsymbol{\mu}) \geq \lambda_h(\boldsymbol{\mu}) \geq \lambda(\boldsymbol{\mu}) \quad \forall \boldsymbol{\mu} \in \mathcal{D}.$$

Let us denote by $\{\zeta_i\}_{i=1}^N$ an orthonormal basis for the space V_N , $N = 1, \dots, N_{\max}$; then, problem (3.1) can be equivalently rewritten as

$$\begin{aligned} A_N \mathbf{U}_N &= \lambda_N B_N(\boldsymbol{\mu}) \mathbf{U}_N, \\ \mathbf{U}_N^T B_N(\boldsymbol{\mu}) \mathbf{U}_N &= 1, \end{aligned} \quad (3.3)$$

where

$$(A_N)_{ij} = a(\zeta_j, \zeta_i), \quad (B_N)_{ij}(\boldsymbol{\mu}) = b(\zeta_j, \zeta_i; \boldsymbol{\mu})$$

and $\mathbf{U}_N(\boldsymbol{\mu}) \in \mathbb{R}^N$ is the vector of degrees of freedom corresponding to the RB solution $u_N(\boldsymbol{\mu}) = \sum_{i=1}^N (\mathbf{U}_N(\boldsymbol{\mu}))_i \zeta_i$.

In order to build up the reduced basis functions $\{\zeta_i\}_{i=1}^N$, we take advantage of a *greedy* algorithm, for which the availability of a *a posteriori* error estimate $\Delta_N^{\text{rel}}(\boldsymbol{\mu})$ on the relative error, fulfilling

$$\frac{\|\nabla u_N(\cdot; \boldsymbol{\mu}) - \nabla u_h(\cdot; \boldsymbol{\mu})\|}{\|\nabla u_N(\cdot; \boldsymbol{\mu})\|} \leq \Delta_N^{\text{rel}}(\boldsymbol{\mu}) \quad \forall \boldsymbol{\mu} \in \mathcal{D}, \quad (3.4)$$

plays a crucial role (see Sect. 4). In particular, given a finite sample $\Xi_{\text{train}} \subset \mathcal{D}$ of (very large) dimension n_{train} , at each iteration N the greedy algorithm selects as a snapshot, among all possible candidates $\boldsymbol{\mu} \in \Xi_{\text{train}}$, the one with largest associated *a posteriori* error bound $\Delta_N^{\text{rel}}(\boldsymbol{\mu})$ and adds it to the space V_N (see Algorithm 3.1). A Gram–Schmidt orthonormalization of the selected snapshot at each step, with respect to previously selected basis functions, is performed to obtain orthonormal RB functions $\{\zeta_1, \dots, \zeta_N\}$. Hence, by construction $\dim(V_N) = N$ and the spaces $\{V_N, N \geq 1\}$ are nested, that is, $V_N \supset V_{N-1}$, $N \geq 1$. We also denote by N_{\max} the maximum admissible dimension of the RB spaces we build; once the space construction has been performed, by restricting to the first $N \leq N_{\max}$ RB functions, we obtain the corresponding N -dimensional RB space V_N .

Since each step of Algorithm 3.1 requires the evaluation of $\Delta_N^{\text{rel}}(\boldsymbol{\mu})$ for any $\boldsymbol{\mu} \in \Xi_{\text{train}}$, it is crucial that this computation could be carried out inexpensively and independently of any quantity related with the high-fidelity approximation $u_h(\boldsymbol{\mu})$. This issue will be addressed in Section 4.3.

Remark 3.3. Other criteria than (3.4) can be chosen for the selection of the retained snapshots during the greedy algorithm. For instance, one could choose to evaluate the L^2 relative error in the eigenfunction, or to consider the relative error in the eigenvalue; however, as we will see in Theorem 4.3, both these quantities can be bounded by suitable powers of $\Delta_N^{\text{rel}}(\boldsymbol{\mu})$.

Algorithm 3.1. Greedy algorithm to build up the reduced space V_N .

Given $\Xi_{\text{train}} \subset \mathcal{D}$, $tol \in (0, 1)$, $maxit \in \mathbb{N}$, $\boldsymbol{\mu}^1 \in \Xi_{\text{train}}$
 Initialize $\mathcal{Z}_0 = \emptyset$, $N = 0$, $\eta^0 = 1$
while $N \leq maxit$ **and** $\eta^N > tol$ **do**
 $N = N + 1$
 Compute the solution $u_h(\boldsymbol{\mu}^N)$ to problem (2.7)
 $\zeta_N = u_h(\boldsymbol{\mu}^N) - \sum_{i=1}^{N-1} (u_h(\boldsymbol{\mu}^N), \zeta_i) \zeta_i$, $\zeta_N = \zeta_N / \|\zeta_N\|$
 $\mathcal{Z}_N = \mathcal{Z}_{N-1} \cup \{\zeta_N\}$
 $\boldsymbol{\mu}^{N+1} = \operatorname{argmax}_{\boldsymbol{\mu} \in \Xi_{\text{train}}} \Delta_N^{\text{rel}}(\boldsymbol{\mu})$
 $\eta^N = \Delta_N^{\text{rel}}(\boldsymbol{\mu}^{N+1})$
end while
 $V_N = \operatorname{span}(\mathcal{Z}_N)$, $N_{\text{max}} = N$

The construction of the RB space is actually performed at an algebraic level. At each step, the vector ζ_N of the degrees of freedom corresponding to the N th basis function, $N = 1, \dots, N_{\text{max}}$, is computed and stored as a column of a rectangular matrix Z . This matrix allows to write the algebraic operators involved in the reduced-order problem (3.1) in terms of those defining problem (2.8), as follows

$$A_N = Z^T A Z, \quad B_N(\boldsymbol{\mu}) = Z^T B(\boldsymbol{\mu}) Z. \tag{3.5}$$

Clearly, $Z Z^T$ represents the projector from V_h to V_N . In order to setup a very efficient RB method, assembling and solving the RB problem must be a very cheap operation. Indeed, assembling the matrix A_N , which actually is $\boldsymbol{\mu}$ -independent, is straightforward. On the other hand, in the case of the $\boldsymbol{\mu}$ -dependent matrix $B_N(\boldsymbol{\mu})$, we can rely on the assumption of affine parametric dependence (2.15), which can be expressed from an algebraic standpoint as

$$B(\boldsymbol{\mu}) = \sum_{k=1}^Q \Theta_k(\boldsymbol{\mu}) B^k, \tag{3.6}$$

where $B_{ij}^k = b_k(\zeta_j, \zeta_i)$. This reflects on the RB matrix $B_N(\boldsymbol{\mu})$, which indeed can be expressed as

$$B_N(\boldsymbol{\mu}) = \sum_{k=1}^Q \Theta_k(\boldsymbol{\mu}) B_N^k, \quad B_N^k = Z^T B^k Z. \tag{3.7}$$

Like the matrix A_N , the matrices B_N^k are $\boldsymbol{\mu}$ -independent and can be assembled once for all in the offline phase. Therefore, for any new value of $\boldsymbol{\mu}$ in the online phase, assembling $B_N(\boldsymbol{\mu})$ requires only the evaluation of the scalar functions $\Theta_k(\boldsymbol{\mu})$ and the linear combination of the Q matrices $B_N^k \in \mathbb{R}^{N \times N}$, which is a very inexpensive operation.

4. A POSTERIORI ERROR ESTIMATES

As shown in Section 3, the construction of a RB approximation through a greedy algorithm relies on suitable *a posteriori* error estimates. The goal of this section is to construct DWR type *a posteriori* estimates for the approximation error between the RB solution $(u_N(\boldsymbol{\mu}), \lambda_N(\boldsymbol{\mu}))$ to problem (3.1) and the high-fidelity solution $(u_h(\boldsymbol{\mu}), \lambda_h(\boldsymbol{\mu}))$ to problem (2.7). To this aim, we follow some ideas employed in [16] (see also [4]). For the sake of simplicity, hereafter the dependence on $\boldsymbol{\mu}$ will be often omitted.

4.1. Main result and preliminaries for its proof

The DWR method (see, e.g., [3] for a general introduction) aims at estimating the error with respect to output functionals depending on the solution of a differential problem. Therefore, let $j : V_h \rightarrow \mathbb{R}$ be a functional

of interest, and let us introduce the parameter-dependent subspace $W_h(\boldsymbol{\mu}) = \text{span}\{u_h(\boldsymbol{\mu})\}^{\perp_b} \subset V_h$, b -orthogonal to the first eigenfunction $u_h(\boldsymbol{\mu})$ of problem (2.7). Then, we define the following as the dual problem related to j : given $\boldsymbol{\mu} \in \mathcal{D}$ and the solution $(\lambda_h(\boldsymbol{\mu}), u_h(\boldsymbol{\mu}))$ to problem (2.7), find $w_h = w_h(\boldsymbol{\mu}) \in W_h(\boldsymbol{\mu})$ such that

$$a(\psi_h, w_h) - \lambda_h(\boldsymbol{\mu})b(\psi_h, w_h; \boldsymbol{\mu}) = j(u_h(\boldsymbol{\mu}))b(\psi_h, u_h(\boldsymbol{\mu}); \boldsymbol{\mu}) - j(\psi_h) \quad \forall \psi_h \in W_h(\boldsymbol{\mu}). \quad (4.1)$$

In order to prevent the dual solution $w_h(\boldsymbol{\mu})$ from having a component in the eigenspace associated to λ_h we require $w_h(\boldsymbol{\mu})$ to be b -orthogonal to $u_h(\boldsymbol{\mu})$, that is $w_h(\boldsymbol{\mu}) \in W_h(\boldsymbol{\mu})$. In this way, the dual problem (4.1) has a unique solution.

Remark 4.1. The subspace $W_h(\boldsymbol{\mu})$ appears in the dual problem (4.1) also as the test space. This is not necessary, since any further test $v_h \in V_h \setminus W_h(\boldsymbol{\mu})$ can be written as $v_h = \psi_h + \alpha u_h(\boldsymbol{\mu})$ for some $\alpha \in \mathbb{R}$, where $\psi_h \in W_h(\boldsymbol{\mu})$ and $u_h(\boldsymbol{\mu})$ is the eigenfunction of the original problem (2.7). Indeed, due to the expression of the right-hand side of the dual problem, and $u_h(\boldsymbol{\mu})$ being the eigenfunction related to $\lambda_h(\boldsymbol{\mu})$, the dual problem itself becomes a tautology when tested against $\alpha u_h(\boldsymbol{\mu})$ for any α . Therefore, taking V_h as a function space is totally equivalent to taking $W_h(\boldsymbol{\mu})$.

Starting from the solution $(\lambda_N(\boldsymbol{\mu}), u_N(\boldsymbol{\mu}))$ of problem (3.1), we can introduce the RB approximation of problem (4.1) as follows:

$$a(\psi_N, w_N) - \lambda_N(\boldsymbol{\mu})b(\psi_N, w_N; \boldsymbol{\mu}) = j(u_N(\boldsymbol{\mu}))b(\psi_N, u_N(\boldsymbol{\mu}); \boldsymbol{\mu}) - j(\psi_N) \quad \forall \psi_N \in W_N(\boldsymbol{\mu}), \quad (4.2)$$

with $W_N(\boldsymbol{\mu}) = \text{span}\{u_N(\boldsymbol{\mu})\}^{\perp_b}$, and where the (unique) solution w_N clearly depends on $\boldsymbol{\mu}$. Moreover, let us introduce the primal and the dual residuals⁵, that is, the residual of the RB approximation for both the primal (3.1) and the dual (4.2) RB problems:

$$\begin{aligned} r(\lambda_N, u_N; \boldsymbol{\mu})(\psi_h) &= a(u_N, \psi_h) - \lambda_N b(u_N, \psi_h; \boldsymbol{\mu}) & \forall \psi_h \in V_h, \\ r^*(\lambda_N, u_N, w_N; \boldsymbol{\mu})(\psi_h) &= a(\psi_h, w_N) - \lambda_N b(\psi_h, w_N; \boldsymbol{\mu}) & \\ &\quad - j(u_N)b(\psi_h, u_N; \boldsymbol{\mu}) + j(\psi_h) & \forall \psi_h \in W_h, \end{aligned} \quad (4.3)$$

respectively. Let us denote by

$$\|r(\lambda_N, u_N; \boldsymbol{\mu})\|_{V_h'} = \sup_{\psi_h \in V_h} \frac{r(\lambda_N, u_N; \boldsymbol{\mu})(\psi_h)}{\|\nabla \psi_h\|}, \quad (4.4)$$

$$\|r^*(\lambda_N, u_N, w_N; \boldsymbol{\mu})\|_{W_h'} = \sup_{\psi_h \in W_h} \frac{r^*(\lambda_N, u_N, w_N; \boldsymbol{\mu})(\psi_h)}{\|\nabla \psi_h\|}, \quad (4.5)$$

the dual norm (with respect to the Hilbert spaces V_h, W_h , endowed with the H^1 -seminorm) of both the primal and the dual residual, respectively. Before stating the main result of the paper, we need to introduce a further assumption.

Assumption 4.2 (Saturation condition). For any $\boldsymbol{\mu} \in \mathcal{D}$, and for any sufficiently large N ,

$$\max\{|\lambda_N(\boldsymbol{\mu}) - \lambda_h(\boldsymbol{\mu})|, \|u_N(\boldsymbol{\mu}) - u_h(\boldsymbol{\mu})\|_b\} < 1. \quad (4.6)$$

Although it might look quite restrictive, this assumption is instrumental for the proof of our main result, and it generally holds in the numerical tests we performed, for which a very rapid convergence is shown to occur – that is, the eigenvalue error rapidly decreases to values smaller than 1, for increasing N .

⁵The dual residual will not be explicitly used in the present paper: it is employed in the proof of Proposition 4.6.

The main result is stated in the following theorem:

Theorem 4.3. *Let $(\lambda_h(\boldsymbol{\mu}), u_h(\boldsymbol{\mu}))$ and $(\lambda_N(\boldsymbol{\mu}), u_N(\boldsymbol{\mu}))$ be the solutions to problems (2.7) and (3.1), respectively, and let us define the following (inf-sup) stability factor of the dual problem (4.1):*

$$\beta_h(\boldsymbol{\mu}) = \inf_{\psi_h \in W_h(\boldsymbol{\mu})} \sup_{\varphi_h \in W_h(\boldsymbol{\mu})} \frac{a(\psi_h, \varphi_h) - \lambda_h(\boldsymbol{\mu})b(\psi_h, \varphi_h; \boldsymbol{\mu})}{\|\nabla \psi_h\| \|\nabla \varphi_h\|}, \quad (4.7)$$

where $W_h(\boldsymbol{\mu}) = \text{span}\{u_h(\boldsymbol{\mu})\}^{\perp_b} \subset V_h$ is the b -orthogonal subspace to $u_h(\boldsymbol{\mu})$.

Under Assumption 4.2, for a sufficiently large N the following inequalities hold:

$$|\lambda_h(\boldsymbol{\mu}) - \lambda_N(\boldsymbol{\mu})| \leq \Delta_{N,\lambda}^h = C_1 \|r(\lambda_N, u_N; \boldsymbol{\mu})\|_{V_h'}^2, \quad (4.8a)$$

$$\|u_h(\boldsymbol{\mu}) - u_N(\boldsymbol{\mu})\| \leq \frac{1}{\sqrt{\varepsilon_0}} \|u_h(\boldsymbol{\mu}) - u_N(\boldsymbol{\mu})\|_b \leq \Delta_{N,0}^h = \frac{1}{\sqrt{\varepsilon_0}} C_2 \|r(\lambda_N, u_N; \boldsymbol{\mu})\|_{V_h'}, \quad (4.8b)$$

$$\|\nabla(u_h(\boldsymbol{\mu}) - u_N(\boldsymbol{\mu}))\| \leq \Delta_{N,1}^h = C_3 \|r(\lambda_N, u_N; \boldsymbol{\mu})\|_{V_h'}. \quad (4.8c)$$

where

$$\begin{aligned} C_1 &= C_1(c_{\Omega,h}, \varepsilon_\infty, \lambda_h(\boldsymbol{\mu}), \beta_h(\boldsymbol{\mu})), \\ C_2 &= C_2(c_{\Omega,h}, \varepsilon_\infty, \lambda_h(\boldsymbol{\mu}), \beta_h(\boldsymbol{\mu})), \\ C_3 &= C_3(c_{\Omega,h}, \varepsilon_\infty, \lambda_h(\boldsymbol{\mu}), \beta_h(\boldsymbol{\mu})). \end{aligned}$$

Moreover, (4.8a)–(4.8c) still hold by replacing λ_h with λ_N in the constants C_1, C_2, C_3 , thus yielding the a posteriori error bounds $\Delta_{N,\lambda}$, $\Delta_{N,0}$, $\Delta_{N,1}$, respectively.

The estimates (4.8a)–(4.8c) share a similar structure with many a posteriori error bounds for RB problems, as they consist in the product between (a suitable power of) the dual norm of the residual, and a scalar factor which depends on the inverse of the (inf-sup) stability factor. The error bound $\Delta_N = \Delta_{N,1}$ will be employed, after normalization by $\|\nabla u_N(\cdot; \boldsymbol{\mu})\|$, in the implementation of the greedy Algorithm 3.1 for the construction of the RB space. In particular, the efficient evaluation of the (dual norms of) residuals relies on the affine expansion of $\boldsymbol{\mu}$ -dependent operators, as shown, e.g., in [33]. The issue of the evaluation of $\boldsymbol{\mu}$ -dependent stability factors $\beta_h(\boldsymbol{\mu})$ will be instead addressed in Section 4.3.

Remark 4.4. We highlight that the DWR method is exploited as theoretical tool in the proof of Theorem 4.3 to derive the expression of the error estimators, since from a practical standpoint we never have to compute a dual solution, nor assemble a dual reduced basis.

The proof of Theorem 4.3, which will be presented in Section 4.2, is divided in four parts and exploits two auxiliary results, whose proofs can be found in ([16], Prop. 2,3):

Proposition 4.5. *For any $\boldsymbol{\mu} \in \mathcal{D}$, let (λ_N, u_N) be a generalized eigenpair of (3.1) and (λ_h, u_h) an associated eigenpair of (2.7). Then, the following identity holds:*

$$(\lambda_h - \lambda_N)(1 - \sigma_h) = r(\lambda_N, u_N; \boldsymbol{\mu})(u_h - \psi_N) \quad \forall \psi_N \in V_N, \quad (4.9)$$

where $\sigma_h = \frac{1}{2} \|u_h - u_N\|_b^2 = \frac{1}{2} b(u_h - u_N, u_h - u_N; \boldsymbol{\mu})$.

Proposition 4.6. *For any $\boldsymbol{\mu} \in \mathcal{D}$, given a linear functional $j : V_h \rightarrow \mathbb{R}$ and the solution w_h of the associated dual problem (4.1), the following identity holds for any $\psi_N \in V_N$:*

$$\begin{aligned} j(u_h - u_N) &= r(\lambda_N, u_N; \boldsymbol{\mu})(w_h - \psi_N) \\ &\quad + (\lambda_h - \lambda_N)b(u_h - u_N, w_h; \boldsymbol{\mu}) + \frac{1}{2} j(u_h) \|u_h - u_N\|_b^2. \end{aligned} \quad (4.10)$$

Employing the results of this section, we now prove Theorem 4.3. We will implicitly assume that $\beta_h(\boldsymbol{\mu}) > 0$ for any $\boldsymbol{\mu} \in \mathcal{D}$; the validity of this assumption will be discussed in Section 4.3. Moreover, for the sake of simplicity, the dependence of the residual $r(\lambda_N, u_N; \boldsymbol{\mu})(\cdot)$ on the RB eigenpair (λ_N, u_N) and the parameter $\boldsymbol{\mu}$ will be understood.

4.2. Proof of Theorem 4.3

Proof. Inspired by the result in ([16], Prop. 4), we consider four steps.

- (i) We start with an intermediate estimate for the eigenvalue error. Taking $\psi_N = u_N$ in (4.9) and using Cauchy–Schwarz inequality, we obtain

$$|\lambda_h - \lambda_N| \leq \frac{1}{1 - \sigma_h} \|r\|_{V'_h} \|\nabla(u_h - u_N)\| \leq 2 \|r\|_{V'_h} \|\nabla(u_h - u_N)\|, \tag{4.11}$$

where the last inequality holds under Assumption 4.2, which in fact implies $\sigma_h < \frac{1}{2}$.

- (ii) Then, we provide an intermediate estimate for the H^1 -seminorm of the eigenfunction error. To this aim, we apply the DWR technique to the functional

$$j(\psi_h) = (\nabla(u_h - u_N), \nabla\psi_h) \quad \forall \psi_h \in V_h. \tag{4.12}$$

The dual problem (4.1) associated to this functional reads as follows: find $w_h \in W_h$ such that

$$\begin{aligned} a(\psi_h, w_h) - \lambda_h b(\psi_h, w_h) &= (\nabla(u_h - u_N), \nabla u_h) b(\psi_h, u_h) \\ &\quad - (\nabla(u_h - u_N), \nabla\psi_h) \quad \forall \psi_h \in W_h, \end{aligned} \tag{4.13}$$

By exploiting the error representation formula (4.10), we obtain

$$\begin{aligned} \|\nabla(u_h - u_N)\|^2 &= r(w_h - \psi_N) + (\lambda_h - \lambda_N) b(u_h - u_N, w_h) \\ &\quad + \frac{1}{2} (\nabla(u_h - u_N), \nabla u_h) \|u_h - u_N\|_b^2. \end{aligned} \tag{4.14}$$

For the right-hand side of (4.13), we have

$$\begin{aligned} (\nabla(u_h - u_N), \nabla u_h) b(\psi_h, u_h) - (\nabla(u_h - u_N), \nabla\psi_h) \\ \leq (\|\nabla u_h\| \|\psi_h\|_b \|u_h\|_b + \|\nabla\psi_h\|) \|\nabla(u_h - u_N)\| \\ \leq (c_{\Omega,h} \sqrt{\varepsilon_\infty \lambda_h} + 1) \|\nabla(u_h - u_N)\| \|\nabla\psi_h\|, \end{aligned} \tag{4.15}$$

where in the last inequality we have exploited Poincaré inequality in V_h (with constant $c_{\Omega,h} > 0$), and the fact that u_h is a solution of problem (2.7) such that $\|u_h\|_b = 1$.

Thanks to Nečas’ Theorem [27], the solution w_h to (4.13) satisfies the following stability estimate:

$$\|\nabla w_h\| \leq \frac{1 + c_{\Omega,h} \sqrt{\varepsilon_\infty \lambda_h}}{\beta_h} \|\nabla(u_h - u_N)\|. \tag{4.16}$$

Hence, the second term in the right-hand side of (4.14) can be controlled as follows:

$$|(\lambda_h - \lambda_N) b(u_h - u_N, w_h)| \leq c_{\Omega,h} \sqrt{\varepsilon_\infty} \frac{1 + c_{\Omega,h} \sqrt{\varepsilon_\infty \lambda_h}}{\beta_h} |\lambda_h - \lambda_N| \|u_h - u_N\|_b \|\nabla(u_h - u_N)\|. \tag{4.17}$$

Let us now consider the third term in (4.14). It is easy to see that

$$\frac{1}{2} (\nabla(u_h - u_N), \nabla u_h) \|u_h - u_N\|_b^2 \leq \frac{1}{2} \|\nabla(u_h - u_N)\| \|\nabla u_h\| \|u_h - u_N\|_b^2 = \frac{\sqrt{\lambda_h}}{2} \|\nabla(u_h - u_N)\| \|u_h - u_N\|_b^2, \tag{4.18}$$

where we have exploited the fact that u_h is the solution to problem (2.7), so that $\|\nabla u_h\|^2 = \lambda_h b(u_h, u_h) = \lambda_h$. Since the residual vanishes for any $\psi_N \in V_N$, we can also control the residual term in (4.14) as follows:

$$|r(w_h - \psi_N)| = |r(w_h)| \leq \|r\|_{V'_h} \|\nabla w_h\| \leq \frac{1 + c_{\Omega,h} \sqrt{\varepsilon_\infty \lambda_h}}{\beta_h} \|r\|_{V'_h} \|\nabla(u_h - u_N)\|. \tag{4.19}$$

By replacing (4.17)–(4.19) in (4.14), we end up with the following intermediate estimate:

$$\|\nabla(u_h - u_N)\| \leq \frac{1 + c_{\Omega,h}\sqrt{\varepsilon_\infty\lambda_h}}{\beta_h} \left(\|r\|_{V'_h} + c_{\Omega,h}\sqrt{\varepsilon_\infty}|\lambda_h - \lambda_N|\|u_h - u_N\|_b \right) + \frac{\sqrt{\lambda_h}}{2}\|u_h - u_N\|_b^2. \quad (4.20)$$

(iii) This step follows the same arguments exploited in point (ii), but now applied to the functional

$$j(\psi_h) = b(u_h - u_N, \psi_h) \quad \forall \psi_h \in V_h. \quad (4.21)$$

In this case the dual problem reads: find $w_h \in W_h$ such that

$$a(\psi_h, w_h) - \lambda_h b(\psi_h, w_h) = b(u_h - u_N, u_h)b(\psi_h, u_h) - b(u_h - u_N, \psi_h) \quad \forall \psi_h \in W_h, \quad (4.22)$$

The right-hand side of the first equation satisfies the following inequality:

$$b(u_h - u_N, u_h)b(\psi_h, u_h) - b(u_h - u_N, \psi_h) \leq (\|u_h\|_b^2 + 1)\|u_h - u_N\|_b\|\psi_h\|_b \leq 2c_{\Omega,h}\sqrt{\varepsilon_\infty}\|u_h - u_N\|_b\|\nabla\psi_h\|, \quad (4.23)$$

and then, due to Nečas' Theorem, the dual solution satisfies the following stability estimate:

$$\|\nabla w_h\| \leq \frac{2c_{\Omega,h}\sqrt{\varepsilon_\infty}}{\beta_h}\|u_h - u_N\|_b. \quad (4.24)$$

Employing once again the error representation formula (4.10), we obtain

$$\begin{aligned} \|u_h - u_N\|_b &\leq \frac{2c_{\Omega,h}\sqrt{\varepsilon_\infty}}{\beta_h} \left(\|r\|_{V'_h} + c_{\Omega,h}\sqrt{\varepsilon_\infty}|\lambda_h - \lambda_N|\|u_h - u_N\|_b \right) + \frac{1}{2}\|u_h - u_N\|_b^2 \\ &\leq \frac{2c_{\Omega,h}\sqrt{\varepsilon_\infty}}{\beta_h} \left(\|r\|_{V'_h} + c_{\Omega,h}\sqrt{\varepsilon_\infty}|\lambda_h - \lambda_N| \right) + \frac{1}{2}\|u_h - u_N\|_b \end{aligned} \quad (4.25)$$

thanks to Assumption 4.2. Finally, we get

$$\|u_h - u_N\|_b \leq \frac{4c_{\Omega,h}\sqrt{\varepsilon_\infty}}{\beta_h} \left(\|r\|_{V'_h} + c_{\Omega,h}\sqrt{\varepsilon_\infty}|\lambda_h - \lambda_N| \right). \quad (4.26)$$

(iv) We can now obtain the *a posteriori* error bounds (4.8a)–(4.8c) by properly combining the intermediate results obtained in (i)–(iii), namely (4.11), (4.20), and (4.26). Starting from (4.11) and introducing two constants $\eta_1, \eta_2 > 0$ and $\gamma_1 = 1 + c_{\Omega,h}\sqrt{\varepsilon_\infty\lambda_h}, \gamma_2 = 4c_{\Omega,h}\sqrt{\varepsilon_\infty}$, we have

$$\begin{aligned} |\lambda_N - \lambda_h| &\leq 2\|r\|_{V'_h}\|\nabla(u_h - u_N)\| \\ &\stackrel{(4.20)}{\leq} 2\|r\|_{V'_h} \left[\frac{\gamma_1}{\beta_h}\|r\|_{V'_h} + \frac{\gamma_1 c_{\Omega,h}\sqrt{\varepsilon_\infty}}{\beta_h}|\lambda_h - \lambda_N|\|u_h - u_N\|_b + \frac{\sqrt{\lambda_h}}{2}\|u_h - u_N\|_b^2 \right] \\ &\leq 2\frac{\gamma_1}{\beta_h}\|r\|_{V'_h}^2 + \frac{1}{\eta_1}|\lambda_h - \lambda_N|^2 + \left(\eta_1 \frac{\gamma_1^2 c_{\Omega,h}^2 \varepsilon_\infty}{\beta_h^2} \|r\|_{V'_h}^2 + \sqrt{\lambda_h} \|r\|_{V'_h} \right) \|u_h - u_N\|_b^2 \\ &\stackrel{(4.6)}{\leq} \left(2\frac{\gamma_1}{\beta_h} + \eta_1 \frac{\gamma_1^2 c_{\Omega,h}^2 \varepsilon_\infty}{\beta_h^2} \right) \|r\|_{V'_h}^2 + \frac{1}{\eta_1}|\lambda_h - \lambda_N|^2 + \sqrt{\lambda_h} \|r\|_{V'_h} \|u_h - u_N\|_b \\ &\stackrel{(4.26)}{\leq} \left(2\frac{\gamma_1}{\beta_h} + \eta_1 \frac{\gamma_1^2 c_{\Omega,h}^2 \varepsilon_\infty}{\beta_h^2} \right) \|r\|_{V'_h}^2 + \frac{1}{\eta_1}|\lambda_h - \lambda_N|^2 + \frac{\gamma_2 \sqrt{\lambda_h}}{\beta_h} \|r\|_{V'_h} \left(\|r\|_{V'_h} + c_{\Omega,h}\sqrt{\varepsilon_\infty}|\lambda_h - \lambda_N| \right) \\ &\leq \left(2\frac{\gamma_1}{\beta_h} + \eta_1 \frac{\gamma_1^2 c_{\Omega,h}^2 \varepsilon_\infty}{\beta_h^2} + \frac{\gamma_2 \sqrt{\lambda_h}}{\beta_h} + \eta_2 \frac{\gamma_2^2 c_{\Omega,h}^2 \varepsilon_\infty \lambda_h}{4\beta_h^2} \right) \|r\|_{V'_h}^2 + \left(\frac{1}{\eta_1} + \frac{1}{\eta_2} \right) |\lambda_h - \lambda_N|^2. \end{aligned} \quad (4.27)$$

By taking $\eta_1 = \eta_2 = 4$, exploiting again (4.6), and substituting the expressions of γ_1, γ_2 , we obtain:

$$\begin{aligned}
 |\lambda_N - \lambda_h| &\leq 2 \left(2 \frac{1 + 3c_{\Omega,h} \sqrt{\varepsilon_\infty \lambda_h}}{\beta_h} + 4 \frac{c_{\Omega,h}^2 \varepsilon_\infty + 2c_{\Omega,h}^3 \varepsilon_\infty \sqrt{\varepsilon_\infty \lambda_h} + 5c_{\Omega,h}^4 \varepsilon_\infty^2 \lambda_h}{\beta_h^2} \right) \|r\|_{V'_h}^2 \\
 &= C_1(c_{\Omega,h}, \varepsilon_\infty, \lambda_h, \beta_h) \|r\|_{V'_h}^2.
 \end{aligned}
 \tag{4.28}$$

Once the eigenvalue error is controlled thanks to (4.28), an error bound on the eigenfunction (with respect to the b -norm) directly follows from (4.26) and (4.6):

$$\begin{aligned}
 \|u_h - u_N\|_b &\stackrel{(4.6)}{\leq} \frac{4c_{\Omega,h} \sqrt{\varepsilon_\infty}}{\beta_h} \left(\|r\|_{V'_h} + c_{\Omega,h} \sqrt{\varepsilon_\infty} \sqrt{|\lambda_h - \lambda_N|} \right) \\
 &\leq \frac{4c_{\Omega,h} \sqrt{\varepsilon_\infty}}{\beta_h} \left(1 + c_{\Omega,h} \sqrt{\varepsilon_\infty C_1(c_{\Omega,h}, \varepsilon_\infty, \lambda_h, \beta_h)} \right) \|r\|_{V'_h} \\
 &= C_2(c_{\Omega,h}, \varepsilon_\infty, \lambda_h, \beta_h) \|r\|_{V'_h}.
 \end{aligned}
 \tag{4.29}$$

This latter inequality, together with (4.20)–(4.28) and Assumption 4.2, provides the following estimate on the H^1 -norm error of the eigenfunction:

$$\begin{aligned}
 \|\nabla(u_h - u_N)\| &\leq \left(\frac{1 + c_{\Omega,h} \sqrt{\varepsilon_\infty \lambda_h}}{\beta_h} + \frac{\sqrt{\lambda_h}}{2} C_2 + c_{\Omega,h} \sqrt{\varepsilon_\infty} \frac{1 + c_{\Omega,h} \sqrt{\varepsilon_\infty \lambda_h}}{\beta_h} \min\{\sqrt{C_1}, C_2\} \right) \|r\|_{V'_h} \\
 &= C_3(c_{\Omega,h}, \varepsilon_\infty, \lambda_h, \beta_h) \|r\|_{V'_h}.
 \end{aligned}
 \tag{4.30}$$

Since the constants C_1, C_2, C_3 are increasing in their argument λ_h , and λ_h is lower than λ_N (see Rem. 3.2), we can replace λ_h with λ_N in the expressions of C_1, C_2, C_3 . Finally, the estimate (4.8b) follows employing the following relation, holding for any $\psi \in L^2(\Omega)$,

$$\|\psi\|_b = \sqrt{\int_\Omega \varepsilon \psi^2 d\Omega} \geq \sqrt{\varepsilon_0} \|\psi\|.
 \tag{4.31}$$

□

4.3. Efficient evaluation of the (inf-sup) stability factor

In principle, to obtain an *efficiently* computable error bound, we would need to provide an inexpensive, N_h -independent *estimate* of the stability factor $\beta_h(\boldsymbol{\mu})$, which enters in the constants C_1, C_2, C_3 appearing in (4.8a)–(4.8c). In this respect, we first prove that $\beta_h(\boldsymbol{\mu}) > 0$ for any $\boldsymbol{\mu} \in \mathcal{D}$ and then show a possible way to compute a cheap, $\boldsymbol{\mu}$ -dependent approximation of this quantity. We underline that we will be able to provide an approximation, rather than a *rigorous lower bound*, of the stability factor; see, e.g., [25] for a related discussion about heuristic strategies for the approximation of stability factors in (both linear and nonlinear) parametrized PDEs. However, in Section 5 we will numerically show that the resulting approximation is able to enhance the computational efficiency of our RB approach without spoiling its performance.

First of all, we give a more explicit expression for $\beta_h(\boldsymbol{\mu})$, and prove its positiveness:

Lemma 4.7. *For any $\boldsymbol{\mu} \in \mathcal{D}$, let $\beta_h(\boldsymbol{\mu})$ be the corresponding inf-sup constant defined in (4.7). Being $\lambda_h(\boldsymbol{\mu}) = \lambda_h^{(1)}(\boldsymbol{\mu})$ and $\lambda_h^{(2)}(\boldsymbol{\mu})$ the first and second eigenvalues of problem (2.7), it holds that*

$$\beta_h(\boldsymbol{\mu}) = 1 - \frac{\lambda_h^{(1)}(\boldsymbol{\mu})}{\lambda_h^{(2)}(\boldsymbol{\mu})} > 0.
 \tag{4.32}$$

Proof. We begin by proving that the quantity $q(\boldsymbol{\mu}) = 1 - \lambda_h^{(1)}(\boldsymbol{\mu})/\lambda_h^{(2)}(\boldsymbol{\mu})$ is a lower bound for $\beta_h(\boldsymbol{\mu})$. We notice that

$$\begin{aligned}\beta_h(\boldsymbol{\mu}) &= \inf_{\psi_h \in W_h(\boldsymbol{\mu})} \sup_{\varphi_h \in W_h(\boldsymbol{\mu})} \frac{a(\psi_h, \varphi_h) - \lambda_h^{(1)}(\boldsymbol{\mu})b(\psi_h, \varphi_h; \boldsymbol{\mu})}{\|\nabla\psi_h\| \|\nabla\varphi_h\|} \\ &\geq \inf_{\psi_h \in W_h(\boldsymbol{\mu})} \frac{a(\psi_h, \psi_h) - \lambda_h^{(1)}(\boldsymbol{\mu})b(\psi_h, \psi_h; \boldsymbol{\mu})}{\|\nabla\psi_h\|^2},\end{aligned}\quad (4.33)$$

that is, $\beta_h(\boldsymbol{\mu})$ is bounded from below by the principal eigenvalue of the bilinear form $a(\cdot, \cdot) - \lambda_h^{(1)}(\boldsymbol{\mu})b(\cdot, \cdot; \boldsymbol{\mu})$ in the space $W_h(\boldsymbol{\mu})$ endowed with the $H^1(\Omega)$ seminorm. This quantity actually equals $q(\boldsymbol{\mu})$. In fact,

$$\begin{aligned}\inf_{\psi_h \in W_h(\boldsymbol{\mu})} \frac{a(\psi_h, \psi_h) - \lambda_h^{(1)}(\boldsymbol{\mu})b(\psi_h, \psi_h; \boldsymbol{\mu})}{\|\nabla\psi_h\|^2} &= \inf_{\psi_h \in W_h(\boldsymbol{\mu})} \left[1 - \lambda_h^{(1)}(\boldsymbol{\mu}) \frac{b(\psi_h, \psi_h; \boldsymbol{\mu})}{\|\nabla\psi_h\|^2} \right] \\ &= 1 - \lambda_h^{(1)}(\boldsymbol{\mu}) \sup_{\psi_h \in W_h(\boldsymbol{\mu})} \frac{b(\psi_h, \psi_h; \boldsymbol{\mu})}{\|\nabla\psi_h\|^2} = 1 - \lambda_h^{(1)}(\boldsymbol{\mu}) \left(\inf_{\psi_h \in W_h(\boldsymbol{\mu})} \frac{\|\nabla\psi_h\|^2}{b(\psi_h, \psi_h; \boldsymbol{\mu})} \right)^{-1} \\ &= 1 - \frac{\lambda_h^{(1)}(\boldsymbol{\mu})}{\lambda_h^{(2)}(\boldsymbol{\mu})} = q(\boldsymbol{\mu}) > 0,\end{aligned}\quad (4.34)$$

where $q(\boldsymbol{\mu})$ is positive because $\lambda_h^{(1)}(\boldsymbol{\mu})$ is simple and smaller than $\lambda_h^{(2)}(\boldsymbol{\mu})$.

Now, we can show that this lower bound is also an upper bound for $\beta_h(\boldsymbol{\mu})$. Getting back to the definition of the inf-sup constant and taking the second eigenfunction $u_h^{(2)}(\boldsymbol{\mu})$ of problem (2.7) as the argument of the infimum yields

$$\begin{aligned}\beta_h(\boldsymbol{\mu}) &= \inf_{\psi_h \in W_h(\boldsymbol{\mu})} \sup_{\varphi_h \in W_h(\boldsymbol{\mu})} \frac{a(\psi_h, \varphi_h) - \lambda_h^{(1)}(\boldsymbol{\mu})b(\psi_h, \varphi_h; \boldsymbol{\mu})}{\|\nabla\psi_h\| \|\nabla\varphi_h\|} \\ &\leq \sup_{\varphi_h \in W_h(\boldsymbol{\mu})} \frac{a(u_h^{(2)}(\boldsymbol{\mu}), \varphi_h) - \lambda_h^{(1)}(\boldsymbol{\mu})b(u_h^{(2)}(\boldsymbol{\mu}), \varphi_h; \boldsymbol{\mu})}{\|\nabla u_h^{(2)}(\boldsymbol{\mu})\| \|\nabla\varphi_h\|} \\ &= \sup_{\varphi_h \in W_h(\boldsymbol{\mu})} \frac{\left(1 - \frac{\lambda_h^{(1)}(\boldsymbol{\mu})}{\lambda_h^{(2)}(\boldsymbol{\mu})} \right) a(u_h^{(2)}(\boldsymbol{\mu}), \varphi_h)}{\|\nabla u_h^{(2)}(\boldsymbol{\mu})\| \|\nabla\varphi_h\|} \leq q(\boldsymbol{\mu}).\end{aligned}\quad (4.35)$$

Since $q(\boldsymbol{\mu})$ is both an upper and a lower bound for $\beta_h(\boldsymbol{\mu})$, the proof is concluded. \square

Although the previous Lemma provides an explicit and computable expression for $\beta_h(\boldsymbol{\mu})$, evaluating it for any $\boldsymbol{\mu} \in \Xi_{\text{train}}$ during the greedy procedure is out of reach. In fact, this operation would require n_{train} solutions to the high-fidelity problem, thus entailing a computational cost which is even larger than the computation of the snapshots for constructing the reduced basis⁶. Moreover, whenever interested to use the error bounds (4.8a)–(4.8c) to certify *online* the RB approximation, relying on the solution of a high-fidelity problem to estimate the stability factor would be too much expensive.

For these reasons, we replace the inf-sup stability factor $\beta_h(\boldsymbol{\mu})$ with the corresponding RB quantity

$$\tilde{\beta}_N(\boldsymbol{\mu}) = 1 - \frac{\lambda_N^{(1)}(\boldsymbol{\mu})}{\lambda_N^{(2)}(\boldsymbol{\mu})},\quad (4.36)$$

where $\lambda_N^{(1)} = \lambda_N$ and $\lambda_N^{(2)}$ are the first and the second eigenvalue of problem (3.1), respectively.

⁶We recall that the greedy procedure actually computes just N snapshots, corresponding to the retained parameter values at each iteration.

Although not rigorous, the error estimates obtained by replacing $\beta_h(\boldsymbol{\mu})$ with $\tilde{\beta}_N(\boldsymbol{\mu})$ in (4.8a)–(4.8c) are very efficient to compute, since $\tilde{\beta}_N(\boldsymbol{\mu})$ is far less expensive to evaluate than $\beta_h(\boldsymbol{\mu})$, and is a very close approximation to the stability factor: indeed, we will show in Section 5.1.2 that $\tilde{\beta}_N(\boldsymbol{\mu})$, for sufficiently large N , yields a very good estimate for $\beta_h(\boldsymbol{\mu})$. Furthermore, although there is no guaranteed reliability of the approximation (4.36)⁷, numerical results show that replacing $\beta_h(\boldsymbol{\mu})$ with $\tilde{\beta}_N(\boldsymbol{\mu})$ does not affect the accuracy of the error bound, while improving its efficiency.

Remark 4.8. Since the estimates in Theorem 4.3 involve the inf-sup constant β_h , which depends on both the first and the second eigenvalue, we could *in principle* consider as basis functions of V_N not only the first eigenfunctions, for different values of $\boldsymbol{\mu}$, but also the second ones. This choice was adopted in the pioneering work [21], where the reduced space results from the Gram–Schmidt orthonormalization of the set $\{u_h^{(1)}(\boldsymbol{\mu}^i), u_h^{(2)}(\boldsymbol{\mu}^i)\}_{i=1}^{N_{\max}/2}$. In Section 5.1.1 we will see that no practical convenience actually comes from this choice.

Remark 4.9. We point out that the constants C_1, C_2, C_3 appearing in the error bounds (4.8a)–(4.8c) not only involve the inf-sup constant β_h , but also $\varepsilon_\infty, \lambda_N$, and $c_{\Omega, h}$. The first two quantities are not expensive to compute, since ε_∞ is a prescribed datum and the RB eigenvalue λ_N only requires the solution of the RB problem. Since the bilinear form $a(\cdot, \cdot)$ is $\boldsymbol{\mu}$ -independent, evaluating the discrete Poincaré constant $c_{\Omega, h}$ just requires an additional solution to problem (2.7), with $\varepsilon \equiv 1$, thanks to (2.11) and Remark 2.2.

5. NUMERICAL RESULTS

In this section we present some numerical results assessing the theoretical analysis developed so far. By considering three different test cases, we show the convergence properties of the RB space V_N for increasing values of N , inspect the behavior of the (inf-sup) stability factors, and assess the computational performance of the *a posteriori* error estimates introduced in this work. We take into account different kinds of parametric dependence $\varepsilon = \varepsilon(\boldsymbol{\mu})$, arising in applications from different fields. The design of the first test case stems from the field of photonic bandgap structures, where the localization of the eigenfunctions induces a local barrier to the transit of light waves with a wavelength equal to the corresponding eigenvalue (see, *e.g.*, [11]). The other two test cases deal with a nonlinear dependence $\varepsilon = \varepsilon(\boldsymbol{\mu})$, and come from the design of acoustic waveguides, anechoic chambers and soundproof barriers, where the localization of some eigenfunction in specific regions of the domain leads to the dissipation of sound waves whose wavelength is equal to the corresponding eigenvalue [26, 37]. In all these cases, the space V_N is built through the greedy Algorithm 3.1. The high-fidelity approximation of the problem is obtained employing piecewise linear finite elements on a computational mesh made of about 8500 elements; finer meshes have also been taken into account, but no relevant differences have been noticed in the numerical results.

Given any test parameter set $\Xi^* \subset \mathcal{D}$, we define the following quantities, which will be employed to present the convergence results throughout this section:

$$\begin{aligned} Err_1^{\text{rel}} &= \text{avg}_{\boldsymbol{\mu}^i \in \Xi^*} \frac{\|\nabla u_h(\boldsymbol{\mu}^i) - \nabla u_N(\boldsymbol{\mu}^i)\|}{\|\nabla u_N(\boldsymbol{\mu}^i)\|}, & Res_1^{\text{rel}} &= \text{avg}_{\boldsymbol{\mu}^i \in \Xi^*} \frac{\|r(\lambda_N(\boldsymbol{\mu}^i), u_N(\boldsymbol{\mu}^i); \boldsymbol{\mu}^i)\|_{V'_h}}{\|\nabla u_N(\boldsymbol{\mu}^i)\|} \\ Err_0^{\text{rel}} &= \text{avg}_{\boldsymbol{\mu}^i \in \Xi^*} \frac{\|u_h(\boldsymbol{\mu}^i) - u_N(\boldsymbol{\mu}^i)\|}{\|u_N(\boldsymbol{\mu}^i)\|}, & Res_0^{\text{rel}} &= \text{avg}_{\boldsymbol{\mu}^i \in \Xi^*} \frac{\|r(\lambda_N(\boldsymbol{\mu}^i), u_N(\boldsymbol{\mu}^i); \boldsymbol{\mu}^i)\|_{V'_h}}{\|u_N(\boldsymbol{\mu}^i)\|} \\ Err_\lambda^{\text{rel}} &= \text{avg}_{\boldsymbol{\mu}^i \in \Xi^*} \frac{|\lambda_h(\boldsymbol{\mu}^i) - \lambda_N(\boldsymbol{\mu}^i)|}{|\lambda_N(\boldsymbol{\mu}^i)|}, & Res_\lambda^{\text{rel}} &= \text{avg}_{\boldsymbol{\mu}^i \in \Xi^*} \frac{\|r(\lambda_N(\boldsymbol{\mu}^i), u_N(\boldsymbol{\mu}^i); \boldsymbol{\mu}^i)\|_{V'_h}^2}{|\lambda_N(\boldsymbol{\mu}^i)|}, \end{aligned}$$

⁷ Indeed, there is *asymptotic* reliability, as $N \rightarrow N_h$.

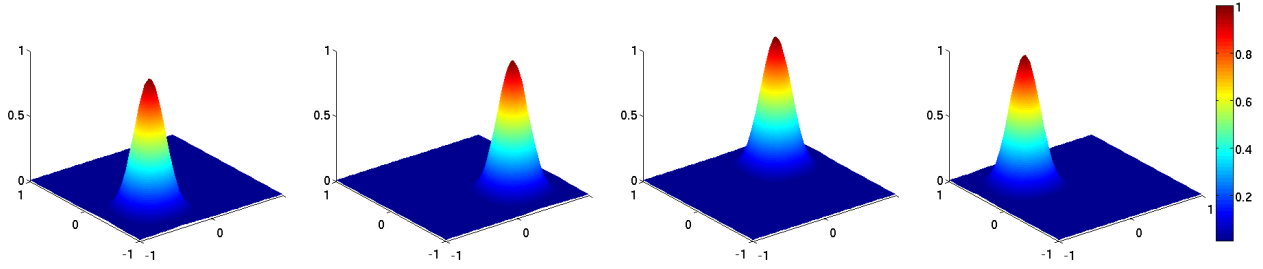


FIGURE 1. Test case 1. The four weight functions $\varepsilon_j(\mathbf{x})$, $j = 1, \dots, 4$.

and

$$\Delta_{N,1}^{\text{rel}} = \text{avg}_{\boldsymbol{\mu}^i \in \Xi^*} \frac{\Delta_{N,1}(\boldsymbol{\mu}^i)}{\|\nabla u_N(\boldsymbol{\mu}^i)\|}, \quad \Delta_{N,0}^{\text{rel}} = \text{avg}_{\boldsymbol{\mu}^i \in \Xi^*} \frac{\Delta_{N,0}(\boldsymbol{\mu}^i)}{\|u_N(\boldsymbol{\mu}^i)\|}, \quad \Delta_{N,\lambda}^{\text{rel}} = \text{avg}_{\boldsymbol{\mu}^i \in \Xi^*} \frac{\Delta_{N,\lambda}(\boldsymbol{\mu}^i)}{|\lambda_N(\boldsymbol{\mu}^i)|} \quad (5.1)$$

where $\Delta_{N,1}, \Delta_{N,0}, \Delta_{N,\lambda}$ are defined in (4.8); $\text{avg}_{\boldsymbol{\mu}^i \in \Xi^*}$ denotes the average on Ξ^* .

The results presented in the following sections assess the validity of the error bounds obtained in Theorem 4.3. Note that, the effectivity of the error bounds, defined as the ratio between the error estimator and the corresponding error, is rather large (ranging between 10^2 to 10^5 , depending of the test case considered). However, poor effectivities are not uncommon in the framework of DWR *a posteriori* analysis [16] and have been found in other RB approximations of eigenvalue problems [10].

5.1. Test case 1. Four-bump weight function

In this first case, we consider the parameter $\boldsymbol{\mu}$ as a point belonging to $\mathcal{D} = [\mu_{\min}, \mu_{\max}]^4 = [10^{-5}, 10^{-2}]^4 \subset \mathbb{R}^4$, with each of its component taking values in the same range. Each component μ_j of $\boldsymbol{\mu}$ is associated to a function $\varepsilon_j(x)$, thus yielding the parametrized weight function $\varepsilon(\boldsymbol{\mu}) = \sum_{j=1}^4 \mu_j \varepsilon_j$. The functions ε_j considered in this test case are chosen as follows:

$$\varepsilon_j(x, y) = 0.01 + \cos(\pi(x - x_{0,j}))^2 \cos(\pi(y - y_{0,j}))^2 e^{-7[(x-x_{0,j})^2 + (y-y_{0,j})^2]} \quad (5.2)$$

with $\mathbf{x}_0 = (-0.4, 0.4, 0.4, -0.4)$, $\mathbf{y}_0 = (-0.4, -0.4, 0.4, 0.4)$, and are plotted in Figure 1. The admissible parameter range has been chosen in order to treat weight functions ε of the same magnitude of those arising in photonic crystals applications (see, e.g., [11]).

Remark 5.1. In definition (5.2), we implicitly set $\varepsilon_0 = 0.01$, $\varepsilon_\infty = 1$. A strictly positive value for ε_0 has been chosen in order to prevent inconsistencies with the theoretical assumptions made in Section 2. Very similar results can be obtained by considering weight functions ε that vanish in some regions of the domain.

In this case, obtaining an affine expansion of the bilinear form $b(\cdot, \cdot; \boldsymbol{\mu})$ under the form (2.15) is straightforward, because the choice (5.2) of the weight functions naturally yields the expansion (2.14) with $Q = 4$ terms. In order to give an insight on the RB space built by the greedy algorithm, we show in Figure 2 some basis functions ζ_n .

Once the RB space has been built, we evaluate the RB approximation *online*, for different parameter values in the admissible range. In Figure 3 we report the RB solution $u_N(\boldsymbol{\mu})$ and the corresponding FE solution $u_h(\boldsymbol{\mu})$ for two representative values of $\boldsymbol{\mu}$. We can see that the relative L^∞ -error on the eigenfunction is on the order of 10^{-5} – this holds for each parameter combination we considered *online* – thus assessing the goodness of the approximation obtained with just $N_{\max} = 27$ basis functions.

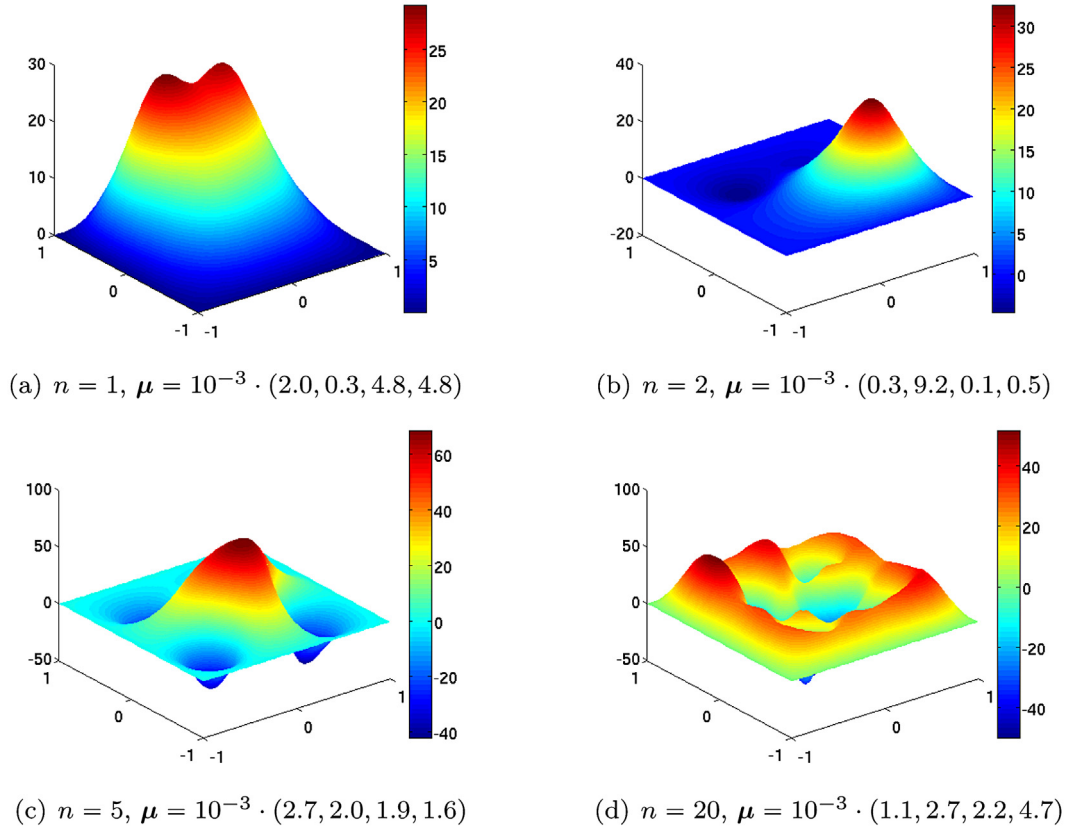


FIGURE 2. Test case 1. Orthonormal basis functions ζ_n for some $n \in \{1, N_{\max} = 27\}$.

5.1.1. Convergence tests

In order to assess the validity of the *a posteriori* error estimates derived in Theorem 4.3, we report some convergence results with respect to the dimension N of the RB space. Aiming at giving, for each N , an evaluation of the RB approximation properties, uniformly on the parameter set \mathcal{D} , we introduce a test set Ξ^* made of 100, randomly chosen elements of \mathcal{D} : for each $\boldsymbol{\mu} \in \Xi^*$ and for each $N \in \{1, 2, \dots, N_{\max}\}$, the approximate eigenpair $(\lambda_N(\boldsymbol{\mu}), u_N(\boldsymbol{\mu}))$ is computed as the principal solution of the reduced problem (3.1) on the space $V_N = \{\zeta_1, \dots, \zeta_N\}$, with $\varepsilon = \sum_{j=1}^4 \mu_j \varepsilon_j$.

This set Ξ^* is also useful to verify empirically if Assumption 4.2 is satisfied, that is to confirm that the current test case lies in the theoretical framework in which the estimates were derived. In particular, in this case we have that, for $N \geq 7$, indeed

$$\max_{\boldsymbol{\mu} \in \Xi^*} \{ |\lambda_N(\boldsymbol{\mu}) - \lambda_h(\boldsymbol{\mu})|, \|u_N(\boldsymbol{\mu}) - u_h(\boldsymbol{\mu})\|_b \} < 1. \tag{5.3}$$

This critical N is the same also for the slightly different cases considered in the forthcoming section 5.1.2.

Throughout this subsection, we consider the residual-based quantities Res_α^{rel} , $\alpha = 0, 1, \lambda$ as (relative) error indicators, temporarily neglecting the contribution of the constants $C_1, C_2/\sqrt{\varepsilon_0}, C_3$ defined in (4.8): the evaluation of the rigorous error bounds $\Delta_{N,\alpha}^{\text{rel}}$, $\alpha = 0, 1, \lambda$, which involves the approximation of the stability factor $\beta_h(\boldsymbol{\mu})$, will be addressed in the next subsection. In particular, we employ the estimator Res_1^{rel} in the basis selection and in the stopping criterion of the greedy algorithm, *i.e.* we apply Algorithm 3.1 with Res_1^{rel} in the place of the generic estimator Δ_N^{rel} .

In Figure 4 (left) we compare the L^2 and H^1 norms of the errors on the eigenfunction, to the residual norm $\|r\|_{V_h'}$, while in Figure 4 (right) we compare the error on the eigenvalue to $\|r\|_{V_h'}^2$. These plots are obtained

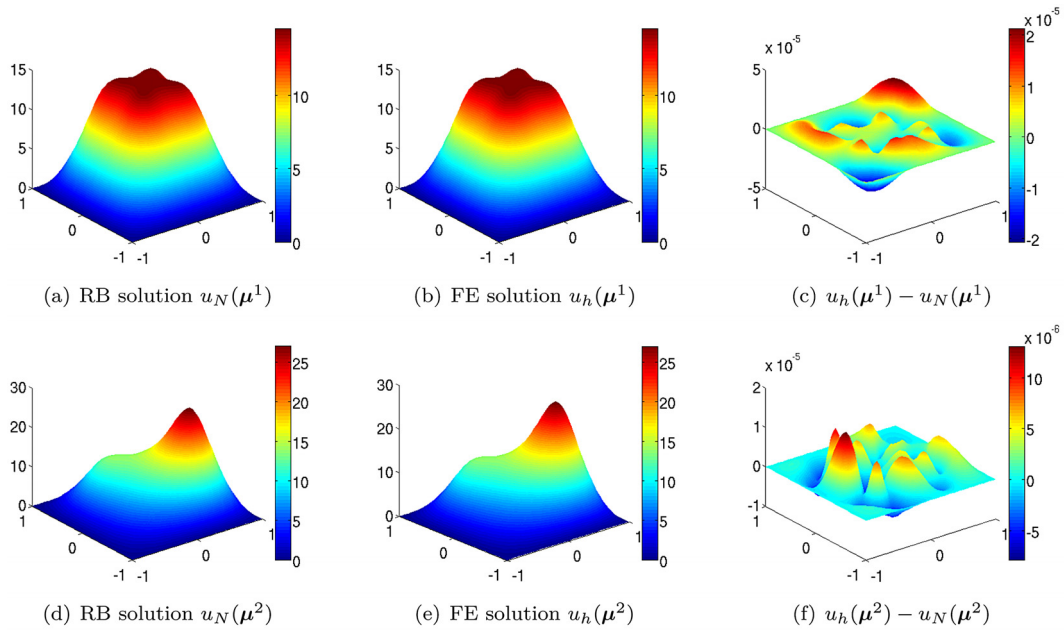


FIGURE 3. Test case 1. Comparison between RB and FE solutions obtained for $\mu^1 = (0.01, 0.01, 0.01, 0.01)$, $\mu^2 = (0.00001, 0.01, 0.001, 0.007)$. The relative error $\|u_N - u_h\|_{L^\infty(\Omega)} / \|u_h\|_{L^\infty}$ is of order of 10^{-5} .

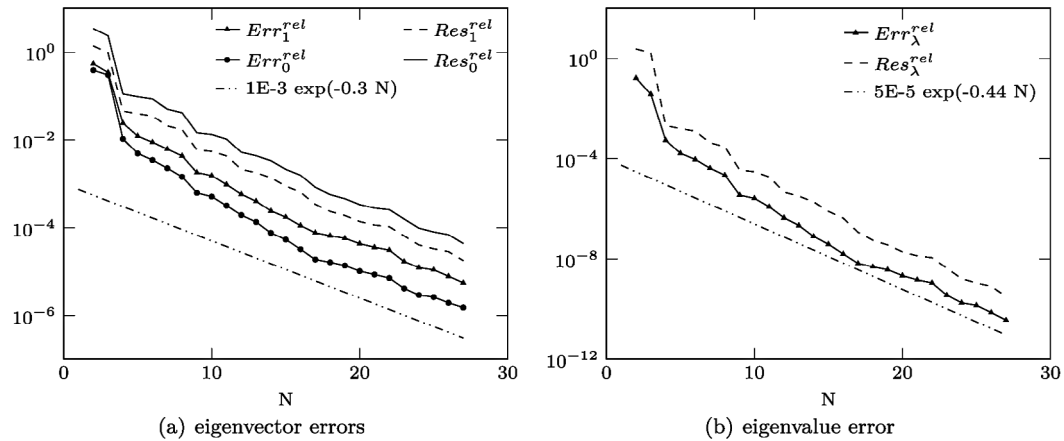


FIGURE 4. Test case 1. Relative errors and corresponding error bounds as functions of $N \in \{1, N_{\max}\}$. In the greedy Algorithm 3.1, the estimator Res_1^{rel} is employed, in the place of Δ_N^{rel} , and the errors are compared to the estimators $Res_1^{rel}, Res_0^{rel}, Res_\lambda^{rel}$, i.e. setting to 1 the constants $C_1, \frac{C_2}{\sqrt{\varepsilon_0}}, C_3$ appearing in $\Delta_{N,\lambda}, \Delta_{N,0}, \Delta_{N,1}$.

in the online phase, once the final RB space $V_{N_{\max}} = \{\zeta_1, \zeta_2, \dots, \zeta_{N_{\max}}\}$ has been completely built. We can observe that the (dual norm of) residuals are very accurate in predicting the trend of the errors. Moreover, the error on the eigenvalue goes with the square of the H^1 -error on the eigenfunction, according to our estimates. This is similar to what happens for linear outputs of the solution of elliptic PDEs (see, e.g., [33]). Finally, we point out that the dependence of the errors on the dimension N is exponential; this is consistent with other theoretical results on the *a priori* convergence of greedy algorithms for parametrized elliptic PDEs (see e.g. [5, 6] and the more recent review in [8]).

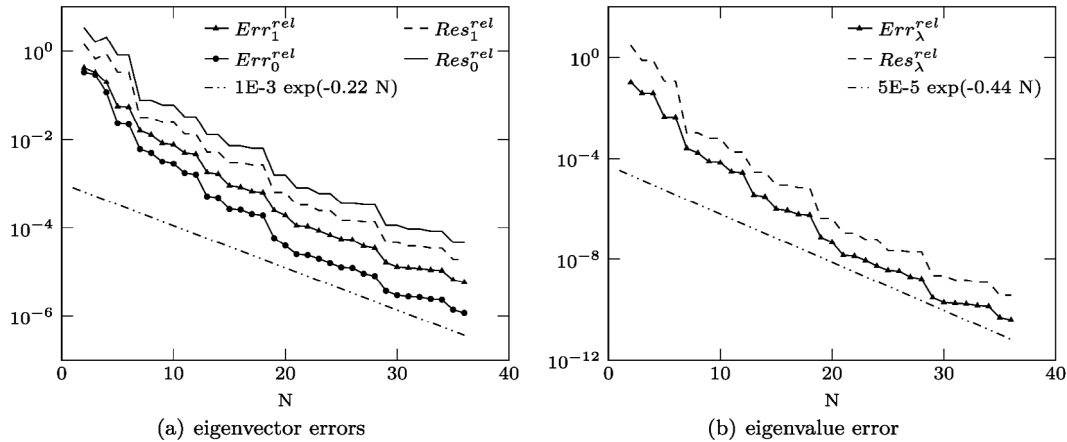


FIGURE 5. Test case 1. Relative errors and corresponding error bounds as functions of $N \in \{1, N_{\max}\}$. For each retained parameter value during the greedy algorithm, the first two eigenfunctions are included in the RB space. In the greedy Algorithm 3.1, the estimator Res_1^{rel} is employed, in the place of Δ_N^{rel} , and the errors are compared to the estimators $Res_1^{rel}, Res_0^{rel}, Res_\lambda^{rel}$, i.e. setting to 1 the constants $C_1, \frac{C_2}{\sqrt{\varepsilon_0}}, C_3$ appearing in $\Delta_{N,\lambda}, \Delta_{N,0}, \Delta_{N,1}$.

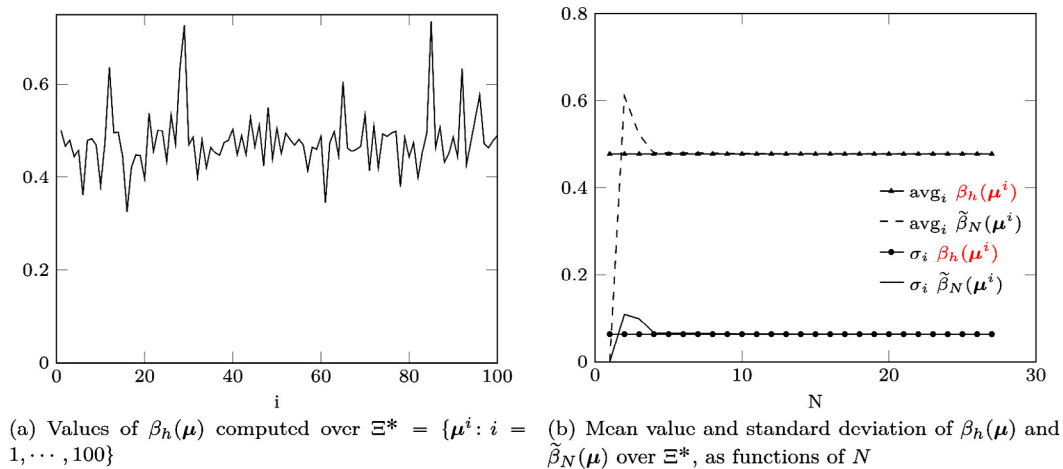


FIGURE 6. Test case 1. Comparison between $\beta_h(\mu)$ and $\tilde{\beta}_N(\mu)$.

We also built the RB space by considering both the first and the second eigenfunction (see Rem. 4.8). This choice does not yield significant improvements in the RB approximation of the solution to problem (2.7): the number of basis functions necessary to fulfill the stopping criterion of the greedy algorithm is much higher ($2N_{\max} = 36$ functions, obtained in 18 iterations, against the 27 basis functions obtained when retaining only $u_h^{(1)}$ at each step) and the convergence of the error is even slower, as one can see by comparing Figure 5 with Figure 4.

5.1.2. Inspecting the inf-sup constant β_h

Let us now explore the effects on the RB algorithm of employing the approximated stability factor $\tilde{\beta}_N(\mu)$ in the computation of the *a posteriori* error bounds (5.1) (see also Sect. 4.3).

First of all, let us evaluate the stability factor $\beta_h(\mu)$ over the test sample Ξ^* . As we can see from Figure 6a, this quantity undergoes slight variations with respect to the parameters μ . We then compare the estimate

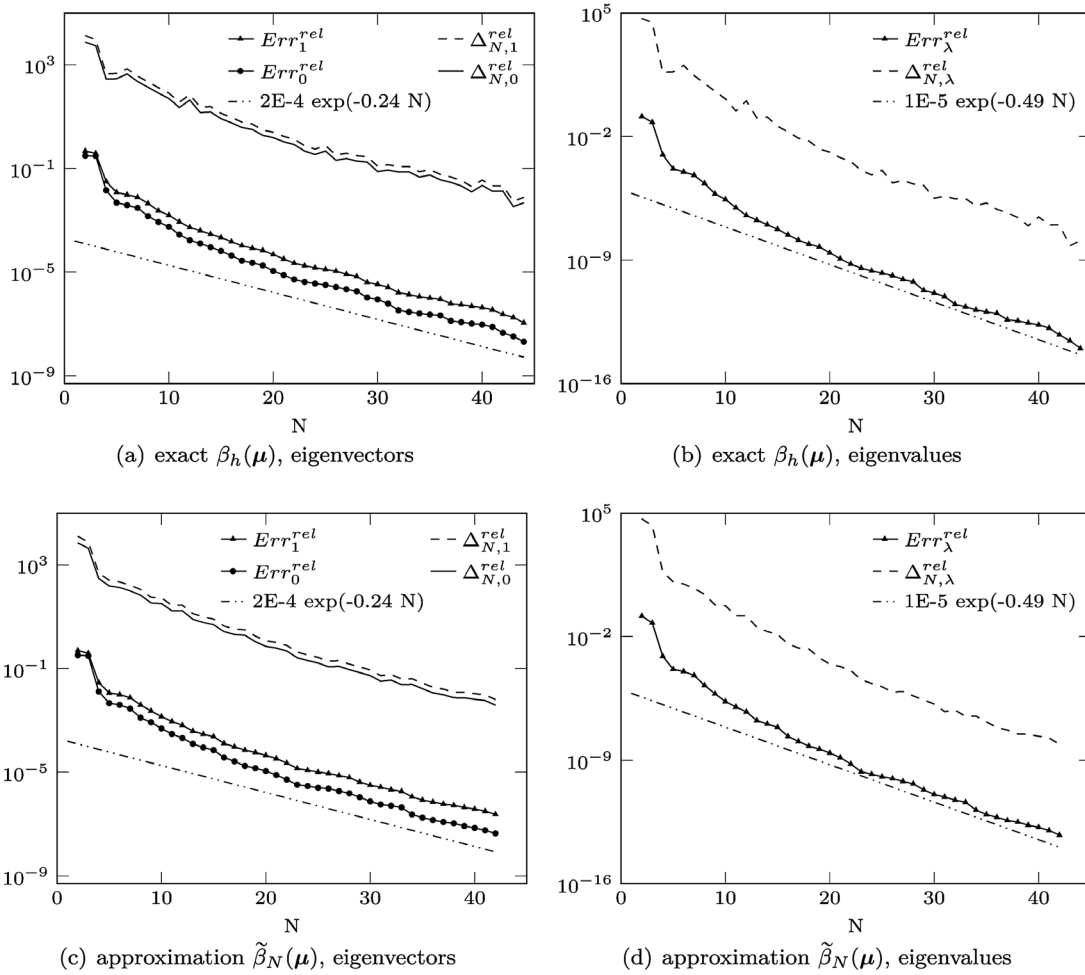


FIGURE 7. Test case 1. Relative errors and corresponding error bounds obtained by considering the inf-sup factor $\beta_h(\boldsymbol{\mu})$ (top) and the approximation $\tilde{\beta}_N(\boldsymbol{\mu})$ (bottom) in the estimators.

$\tilde{\beta}_N(\boldsymbol{\mu})$ with $\beta_h(\boldsymbol{\mu})$: by taking the mean and the standard deviation over Ξ^* , and plotting these two quantities as functions of N (Fig. 6b), we can see that $\tilde{\beta}_N(\boldsymbol{\mu})$ provides (i) a positive estimate to the inf-sup factor; and (ii) a very good approximation to $\beta_h(\boldsymbol{\mu})$. This is rather evident by observing that the standard deviations of $\beta_h(\boldsymbol{\mu})$ and $\tilde{\beta}_N(\boldsymbol{\mu})$ over Ξ^* are about one tenth of their mean values. We can see that $\tilde{\beta}_N(\boldsymbol{\mu})$ is a reliable approximation of $\beta_h(\boldsymbol{\mu})$ for $N > 4$, both in the mean value and in the standard deviation (this latter evaluated with respect to $\boldsymbol{\mu}$ variations). Hence, $\tilde{\beta}_N(\boldsymbol{\mu})$ represents a good (and inexpensive) approximation of the inf-sup constant $\beta_h(\boldsymbol{\mu})$, which is indeed used in the error estimates (4.8).

Then we investigate the impact of the use of $\tilde{\beta}_N(\boldsymbol{\mu})$ on the construction of the RB space, and on the consequent *online* evaluation of the RB approximation. The convergence results reported in Figure 7 (and similarly for the ones presented in the following sections) are obtained basing both the stopping criterion of the greedy algorithm and the basis selection on the relative error estimators (5.1) involving either the *rigorous* inf-sup constant β_h (Figs. 7a and 7b), or its surrogate $\tilde{\beta}_N$ (Figs. 7c and 7d). We find an almost exact correspondence between the results reported in these plots – negligible discrepancies are due to the different error bounds – so that we can confirm that the estimate (4.36) of the (inf-sup) stability factor is absolutely acceptable, and yields very

accurate error bounds. Therefore, the computable quantity $\widetilde{\beta}_N(\boldsymbol{\mu})$ seems to be a very good candidate to replace the (computationally unaffordable) stability factor $\beta_h(\boldsymbol{\mu})$, and hence in the following sections we always employ $\widetilde{\beta}_N$ in the computation of the estimators.

5.2. Test cases 2 and 3. A two-phase drum

In this section we consider a weight function of the form

$$\varepsilon(\mathbf{x}; \boldsymbol{\mu}) = \varepsilon_1 \chi_{\Omega_1(\boldsymbol{\mu})}(\mathbf{x}) + \varepsilon_2 \chi_{\Omega_2(\boldsymbol{\mu})}(\mathbf{x}), \quad (5.4)$$

with $\Omega_1(\boldsymbol{\mu}) \cap \Omega_2(\boldsymbol{\mu}) = \emptyset$, $\Omega_1(\boldsymbol{\mu}) \cup \Omega_2(\boldsymbol{\mu}) = \Omega = (-1, 1)^2$, for any admissible $\boldsymbol{\mu}$. The localization of the eigenvalues corresponding to weight functions of the form (5.4) has interesting applications, such as the design of acoustic waveguides [26] or the study of fractal cavities [37] related to the construction of anechoic chambers or acoustic barriers. In this latter case, for example, Ω_1 could represent the region occupied by the barrier, while in Ω_2 there is only air. Considering weight functions of the form (5.4) brings some further difficulties in solving the problem, due to the nonlinear dependence of ε on $\boldsymbol{\mu}$. Indeed, as stated in Section 2.3, the efficiency of the RB approximation stems from the general assumption that the dependence of the problem coefficients on $\boldsymbol{\mu}$ is affine.

In this case we exploit EIM to obtain an affine expansion of the function $\varepsilon(\mathbf{x}; \boldsymbol{\mu})$, where \mathbf{x} and $\boldsymbol{\mu}$ appear as separable variables (see Sect. 2.3). This yields an approximate expression $\widetilde{\varepsilon}(\mathbf{x}, \boldsymbol{\mu})$ as in (2.16) made by the sum of Q terms. As the quality of the EIM approximation of a function can be highly compromised in presence of sharp jumps, we modified in advance the function ε defined in (5.4), introducing a linear transition between ε_1 and ε_2 in a narrow region around the interface separating Ω_1 and Ω_2 . In each test case, an EIM expansion of 100 terms is considered, obtained by requiring the EIM error to be below a tolerance $\varepsilon_{\text{tol}}^{\text{EIM}} = 10^{-3}$. Numerical tests performed with EIM expansions made by a larger number of terms did not yield significantly different results.

Considering the problem obtained through the EIM-approximation of the weight function ε , we can exploit the greedy Algorithm 3.1 to build up the reduced space V_N , basing the choice of the basis functions on the error estimators (5.1), as suggested by the results of the previous section. In the following, we consider the performance of the RB algorithm dealing with two different types of interface separating Ω_1 and Ω_2 .

In both the cases considered below, Assumption 4.2 is verified right away for $N \geq 1$. Therefore, the estimates of Theorem 4.3 are rigorous in these cases.

5.2.1. Test case 2. Sinusoidal interface

As a first kind of interface separating $\Omega_1(\boldsymbol{\mu})$ and $\Omega_2(\boldsymbol{\mu})$, we consider the graph of the function

$$x = \mu_1 \sin(\mu_2 \pi y) + \mu_3 \sin(\mu_4 \pi y), \quad (5.5)$$

with the parameters $\boldsymbol{\mu} = (\mu_1, \mu_2, \mu_3, \mu_4)$ ranging in $\mathcal{D} = ([0.1, 0.2] \times [1, 8])^2$. By choosing $\varepsilon_1 = 0.1, \varepsilon_2 = 0.2$, using definition (5.4) and introducing a linear transition between ε_1 and ε_2 , we obtain the weight function ε , reported in the left column of Figure 8 for different values of $\boldsymbol{\mu}$. For the sake of computational efficiency, we then apply EIM to recover an affine approximation $\widetilde{\varepsilon}$ of the weight function ε . We point out that both the FE solution to (2.7) and its RB approximation are obtained considering the EIM-approximated weight function $\widetilde{\varepsilon}$; hence, the discussion which follows does not deal with the error associated to the EIM approximation.

In Figure 8 we can see that the maximum of the first eigenfunction lays in the domain Ω_2 , which is characterized by a higher value of ε . The figure also shows low sensitivity of the eigenfunction to changes of $\boldsymbol{\mu}$: for higher frequencies of the sinusoidal interface, the maximum of the eigenfunction tends to lay on the line $y = 0$, while for lower frequencies, it slightly moves down, towards values of y where the fraction of the domain occupied by Ω_2 is larger. The RB approximation of dimension $N = 50$ is very close to the FE solution (with a relative error on the order of 10^{-3}).

Good agreement with the theoretical results of the previous section is found also in the convergence graphs of Figure 9, where the quadratic effect of the eigenvalue can be noticed, too. However, in this case the convergence

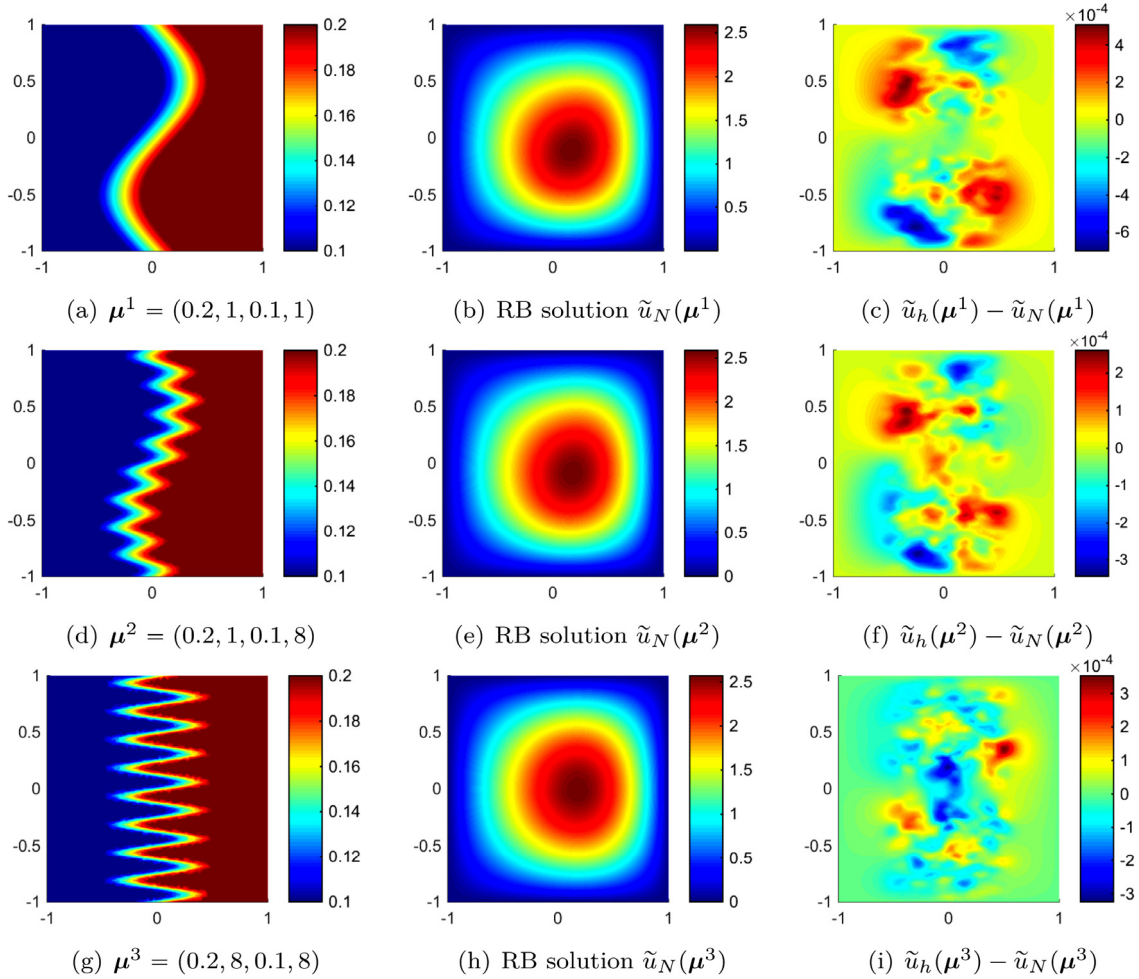


FIGURE 8. Test case 2. Weight functions $\varepsilon(\boldsymbol{\mu})$ (left), RB approximations (center) and errors between RB and FE approximations (right) obtained with the EIM-approximated weight functions $\tilde{\varepsilon}(\boldsymbol{\mu})$, for specific values of $\boldsymbol{\mu}$. The relative error $\|\tilde{u}_N - \tilde{u}_h\|_{L^\infty(\Omega)} / \|\tilde{u}_h\|_{L^\infty}$ (see (c), (f) and (i)) is of order 10^{-4} .

is much slower than in the case of the four-bumps ε of test case 1 considered in Section 5.1. The error in the eigenfunction is about $\exp(-0.031N)$, whereas in the the four-bump case we had found a much faster convergence ($\exp(-0.24N)$, see Fig. 7). Test case 2 is in fact more difficult although we are still dealing with $p = 4$ parameters. Indeed, the presence of μ_2 and μ_4 makes the parametric dependence of $\varepsilon(\cdot; \boldsymbol{\mu})$, as well as that of the solution $u(\boldsymbol{\mu})$, much more involved: the greedy selection of both (i) interpolation points while performing EIM and (ii) snapshots for the RB space construction require several iterations, as it results from the large number ($Q = 100$) of EIM terms and from the convergence plot of Figure 9, respectively.

To show that the slower error convergence comes rather from the *intrinsic* difficulty of the problem than on possible artifacts introduced by our reduction strategy, a comparison between the greedy algorithm and proper orthogonal decomposition (POD) has been carried out; see, e.g., [34] for further details about this alternative technique for the construction of the RB space. Starting from a set of $n_s = 1000$ snapshots (selected through a latin hypercube sampling of the parameter space), we obtain that the singular values of the snapshot matrix show a slow decay similarly to the error bounds evaluated by the greedy algorithm, see Figure 10.

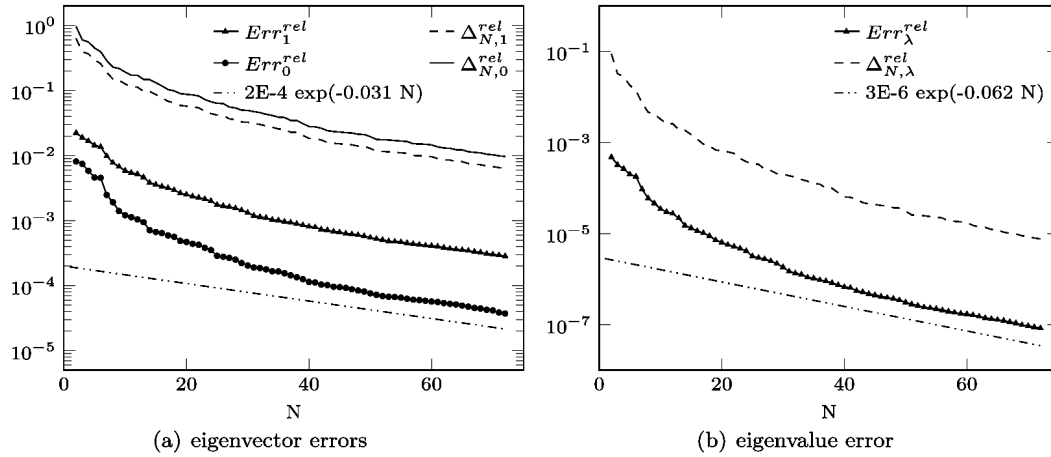


FIGURE 9. Test case 2. Relative errors and corresponding error bounds with respect to the RB space dimension $N \in \{1, N_{\max}\}$.

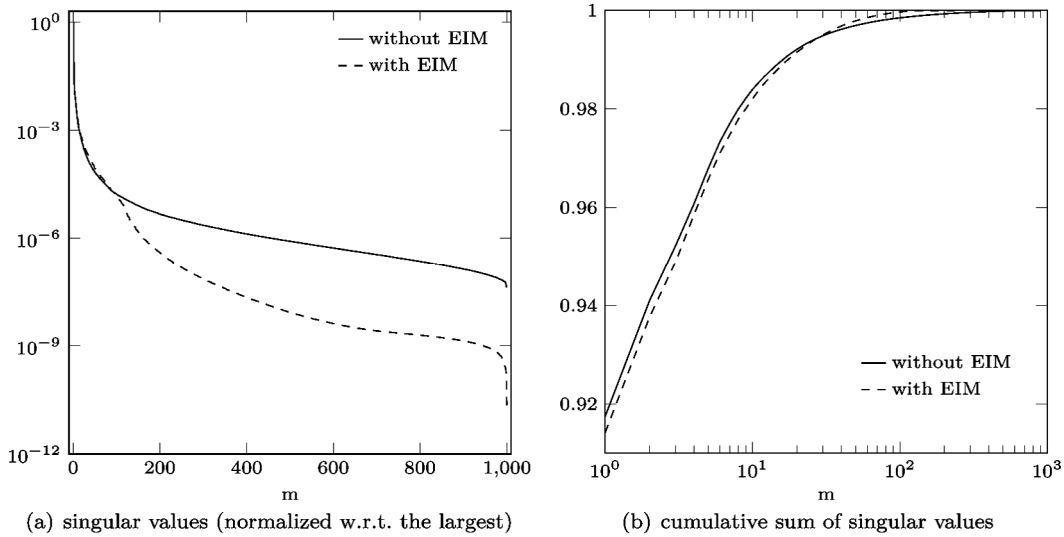


FIGURE 10. Test case 2. POD construction of the RB space from a set of $n_s = 1000$ snapshots, obtained with and without performing EIM ($\varepsilon_{\text{tol}}^{EIM} = 10^{-3}$, $Q = 100$, $\#\Xi_{\text{train}}^{EIM} = 4000$) on the weight function ε .

Note also that the trends of singular values obtained when the snapshots are computed by relying (i) on the original (non-affine) operator or (ii) on its EIM approximation are very similar (see Fig. 10, right). These considerations show that (i) the complexity of the problem is not small, and that (ii) our *a posteriori* error bounds provide a good snapshot selection. In particular, we obtain a degree of accuracy of 2×10^{-3} with $N = 50$ (measured by the sum of the squares of the singular values corresponding to the neglected modes, from $N + 1$ to n_s), see Figure 10. Similarly, we obtain the same degree of accuracy 2×10^{-3} on the relative error through the greedy algorithm by considering $N = 24$ basis functions (for $N = 50$, the greedy algorithm allows to reach a relative error of about 5×10^{-4} ; see, e.g., Fig. 9a).

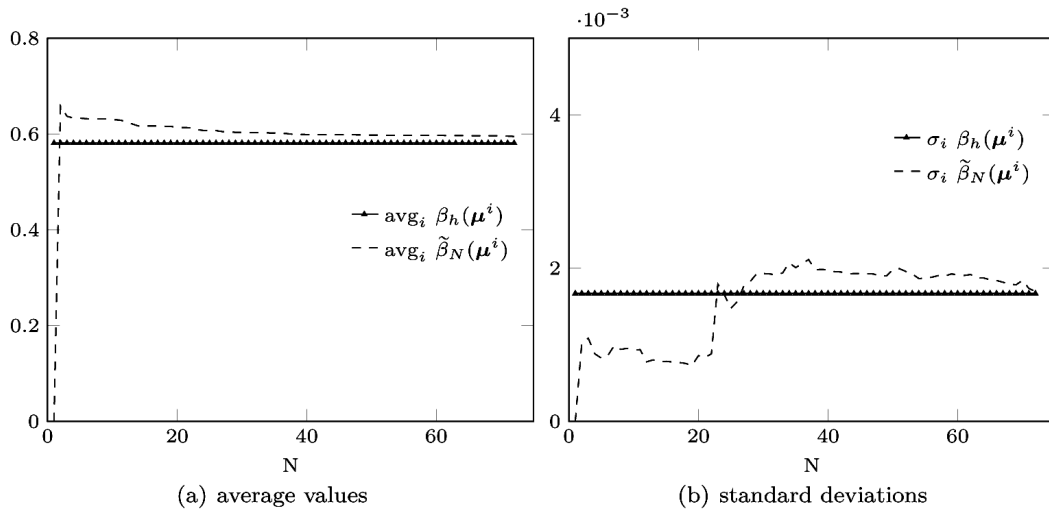


FIGURE 11. Test case 2. Comparison between β_h and $\tilde{\beta}_N$.

In Figure 11 we also report the behaviors of the inf-sup constant $\beta_h(\boldsymbol{\mu})$ and of its estimate $\tilde{\beta}_N(\boldsymbol{\mu})$. The convergence of (the mean value of) $\tilde{\beta}_N(\boldsymbol{\mu})$ towards $\beta_h(\boldsymbol{\mu})$ is much slower than in the previous case (see Fig. 6b): this is in accordance to the slower convergence already noticed in the solution error. On the other hand, negligible differences of $\beta_h(\boldsymbol{\mu})$ and $\tilde{\beta}_N(\boldsymbol{\mu})$ with respect to $\boldsymbol{\mu}$ can be remarked: actually, their standard deviations in the test parameter space Ξ^* are two orders of magnitude smaller than their average values. In order to inspect the error introduced by EIM, we solved the FE problem (2.7) with the exact weight function ε , for different values of $\boldsymbol{\mu}$: the results (not reported for brevity) are indeed very similar to the ones shown in Figure 8, with an L^∞ relative discrepancy smaller than 1%.

5.2.2. Test case 3. Spiral interface

In this section we study the performance of the RB approximation in the case of a non-affinely parametrized function $\varepsilon(\cdot; \boldsymbol{\mu})$ in which the eigenfunction shows to be more sensitive to the variation of the parameters – compare, e.g., the variability of the eigenfunction w.r.t. $\boldsymbol{\mu}$ in Figures 8 and 12. To this aim, we consider an interface between the subregions Ω_1 and Ω_2 that is no more the graph of a function, and is built up using spiral functions under the form

$$\rho(\theta) = \left(\frac{\theta - \mu_1}{\pi - \mu_1} \right)^{\mu_2 + 1}, \quad \theta \in \{\mu_1, \pi\}, \tag{5.6}$$

with $\rho = \sqrt{x^2 + y^2}$, $\theta = \arctan(y/x)$, and then modifying them to obtain shapes like those reported on the left column of Figure 12. We set $\varepsilon_1 = 1, \varepsilon_2 = 10$ and a linear transition is introduced between the two values, as in the previous section. For the interface described by (5.6), the first parameter $\mu_1 \in [0.1, 0.8]$ sets the slope of the curve in $(x, y) = (0, 0)$, while $\mu_2 \in [0, 4]$ basically shrinks the curve in the x direction. EIM is then applied to recover an affinely parametrized expression $\tilde{\varepsilon}$ approximating the weight function ε .

In this case, the eigenfunction is instead more sensitive to parameter variations, as shown in Figure 12, where we can also observe that the RB solution, obtained with $N = 126$ basis functions, provides a very good approximation to the corresponding FE solution.

Looking at the convergence plots of Figure 13, we point out that the convergence speed is on the order of that found in the sinusoidal-interface case, see Figure 9 for a comparison. The similarity with the previous test case can be seen also in the rate of convergence of $\tilde{\beta}_N$ towards the inf-sup constant β_h , see Figure 14 (the marginally

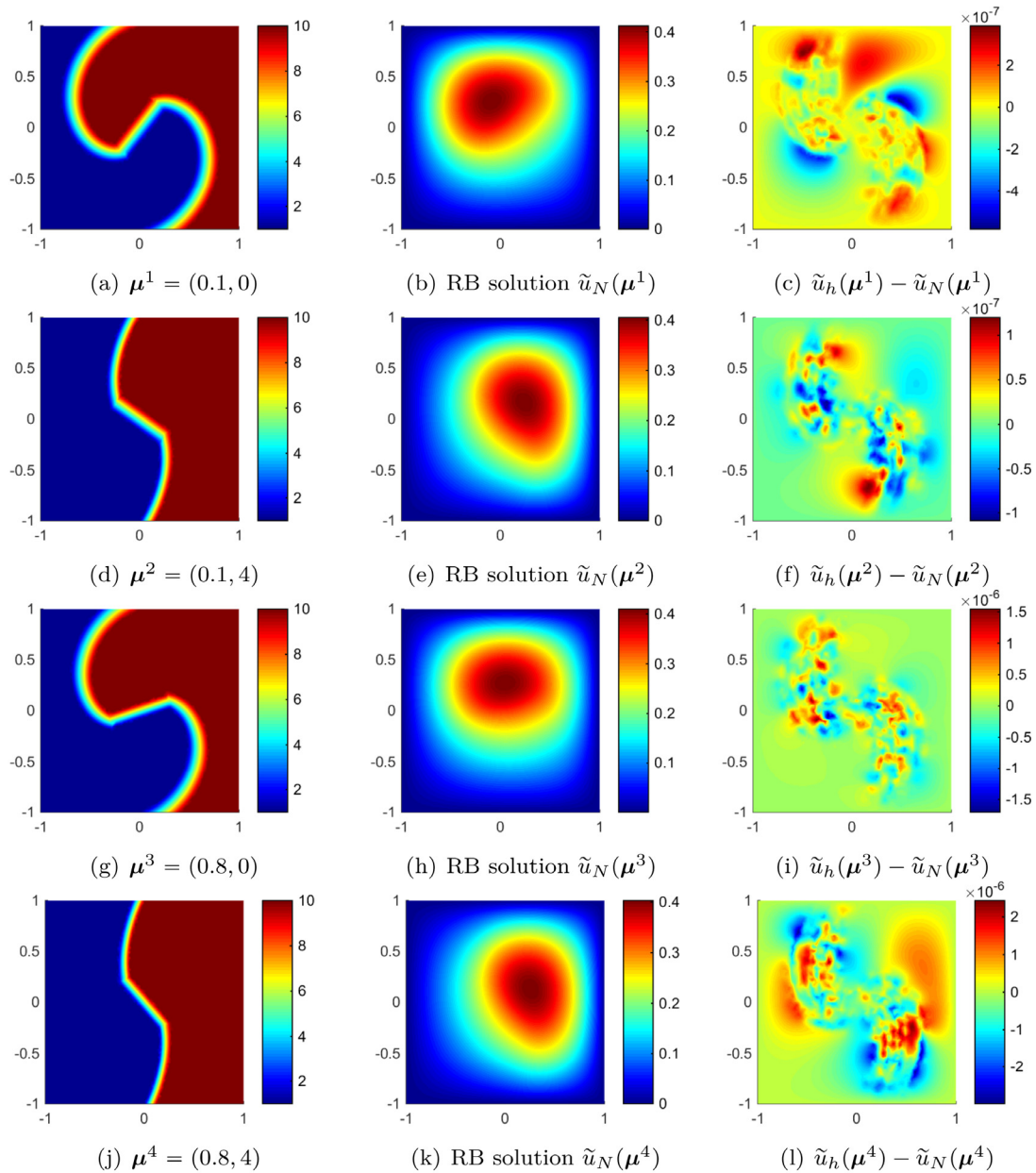


FIGURE 12. Test case 3. Weight functions $\varepsilon(\mu)$ (left), RB approximations (center) and errors between RB and FE approximations (right) obtained with the EIM-approximated weight functions $\tilde{\varepsilon}(\mu)$, for specific values of μ . The L^∞ relative error (see (c), (f), (i) and (l)) is of order 10^{-6} – 10^{-7} .

higher standard deviation observed in this case just comes from the more pronounced parameter-sensitivity of the eigenfunction). Hence, we can conclude that the proposed greedy algorithm enables an efficient construction of a RB approximation also in the case of non-affinely parametrized eigenproblems exhibiting a more pronounced parametric dependence.

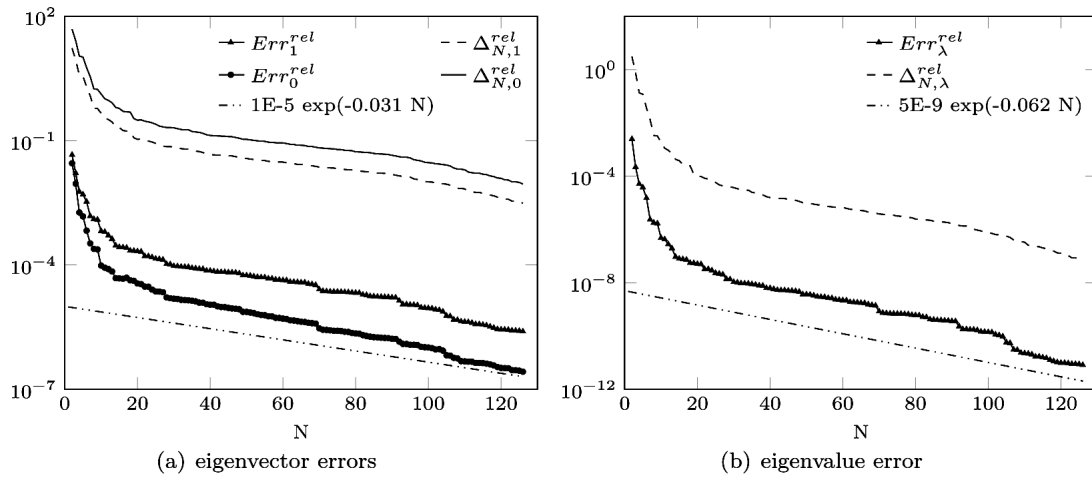


FIGURE 13. Test case 3. Relative errors and corresponding error bounds with respect to the RB space dimension $N \in \{1, N_{\max}\}$.

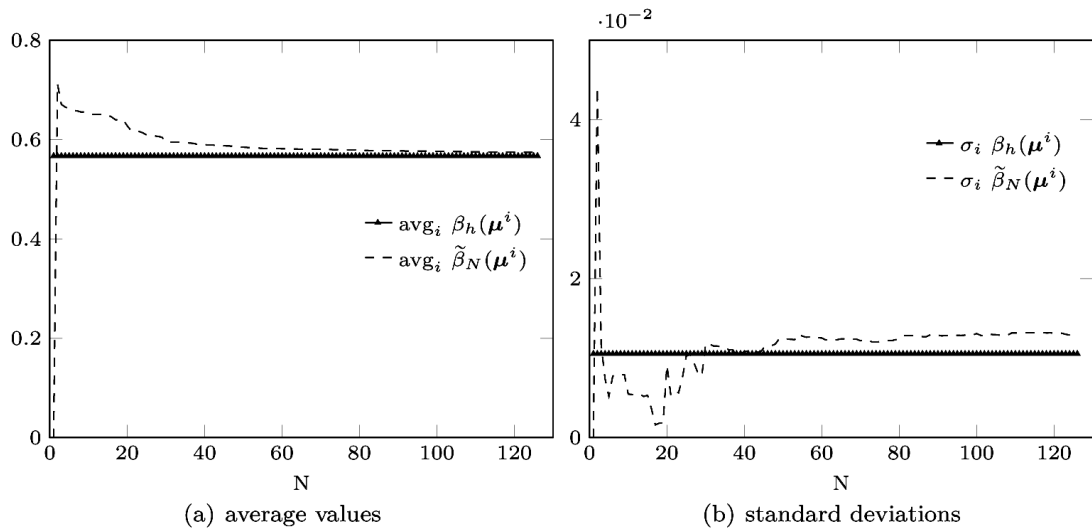


FIGURE 14. Test case 3. Comparison between β_h and its surrogate $\tilde{\beta}_N$.

6. CONCLUSIONS

In this paper we developed a new RB method for the rapid and reliable approximation of parametrized elliptic eigenvalue problems. The method relies on dual weighted residual type *a posteriori* error indicators which estimate, for any value of the parameters, the error between the high-fidelity finite element approximation of the first eigenpair and the corresponding reduced basis approximations. We proved that the proposed error estimators are reliable. Moreover, the *a posteriori* error estimators have been exploited not only to certify the RB approximation with respect to the high-fidelity one, but also to set up a very efficient greedy algorithm for the offline construction of a RB space. In this way, we were able to approximate a parametrized elliptic eigenvalue problem by relying on a very low-dimensional subspace, thus yielding a remarkable computational

speedup. Several numerical experiments (with affine and non-affine parametrizations) showed the validity of the proposed RB approach.

APPENDIX A. AN EXTENSION OF THE BAUER–FIKE THEOREM TO GENERALIZED EIGENPROBLEMS

Given two symmetric positive definite matrices A and B , let $\lambda(A, B)$ be the generalized eigenvalues fulfilling $A\mathbf{x} = \lambda B\mathbf{x}$. There exists a symmetric square root of B , denoted by $B^{1/2}$, such that $B^{1/2}B^{1/2} = B^{1/2}B^{T/2} = B$. Moreover, given the matrix $C = B^{-1/2}AB^{-1/2}$, there exists an orthogonal matrix Q such that $Q^T C Q = \text{diag}(\lambda_1(C), \dots, \lambda_n(C))$, where $\lambda_i(C)$ are the eigenvalues of C . Note that the generalized eigenvalues $\lambda(A, B)$ coincide with $\lambda(C)$.

Introducing the diagonal matrix $D_{A,B} = \text{diag}(\lambda_1(A, B), \dots, \lambda_n(A, B))$, we have

$$Q^T C Q = D_{A,B} \tag{A.1}$$

It is easy to show that the matrix $X = B^{-1/2}Q$ diagonalizes both A and B , indeed

$$\begin{aligned} X^T A X &= (B^{-1/2}Q)^T A B^{-1/2}Q = Q^T B^{-1/2} A B^{-1/2}Q = Q^T C Q = D_{A,B}, \\ X^T B X &= (B^{-1/2}Q)^T B B^{-1/2}Q = Q^T B^{-1/2} B B^{-1/2}Q = Q^T Q = I. \end{aligned} \tag{A.2}$$

An extension of the Bauer–Fike theorem (see, *e.g.* [14], Thm. 7.2.2) to generalized eigenproblems with the perturbation acting only on the B matrix is formulated in the following theorem.

Theorem A.1. *If μ is a generalized eigenvalue of the perturbed problem*

$$A\mathbf{x} = \mu \tilde{B}\mathbf{x}, \tag{A.3}$$

and

$$X^T A X = D_{A,B}, \quad X^T B X = I, \tag{A.4}$$

then

$$\min_{\lambda \in \lambda(A,B)} \frac{|\lambda - \mu|}{|\mu|} \leq \|X^T\|_p \|B - \tilde{B}\|_p \|X\|_p, \tag{A.5}$$

where $\|\cdot\|_p$ denotes any of the p -norms.

Proof. Let us consider the matrix

$$W = X^T(A - \mu \tilde{B})X = D_{A,B} - \mu I - \mu X^T(B - \tilde{B})X.$$

If $\mu \in \lambda(A, B)$ then (A.5) is obviously true. Otherwise, $D_{A,B} - \mu I$ is invertible. Since W is singular, we have, for some $\mathbf{x} \neq \mathbf{0}$:

$$0 = I\mathbf{x} - \mu(D_{A,B} - \mu I)^{-1}X^T(B - \tilde{B})X\mathbf{x}.$$

That is,

$$\mathbf{x} = \mu(D_{A,B} - \mu I)^{-1}X^T(B - \tilde{B})X\mathbf{x}.$$

Since $(D_{A,B} - \mu I)^{-1}$ is diagonal, its p -norm is the absolute value of the largest diagonal entry, thus we have

$$\begin{aligned} \|\mathbf{x}\|_p &\leq |\mu| \|(D_{A,B} - \mu I)^{-1}\|_p \|X^T(B - \tilde{B})X\|_p \|\mathbf{x}\|_p \\ &\leq \frac{|\mu|}{\min_{\lambda \in \lambda(A,B)} |\lambda - \mu|} \|X^T\|_p \|B - \tilde{B}\|_p \|X\|_p \|\mathbf{x}\|_p, \end{aligned} \tag{A.6}$$

completing the proof. □

Acknowledgements. The authors would like to thank the anonymous referees for the careful reading of the manuscript and for their many insightful comments and suggestions.

REFERENCES

- [1] A. Ammar and F. Chinesta, Circumventing curse of dimensionality in the solution of highly multidimensional models encountered in quantum mechanics using meshfree finite sums decomposition. In *Meshfree Methods for Partial Differential Equations IV*, edited by M. Griebel and M. Schweitzer. Vol. 65 of *Lect. Notes Comput. Sci. Eng.* Springer, Berlin, Heidelberg (2008) 1–17.
- [2] M. Barrault, Y. Maday, N.C. Nguyen and A.T. Patera, An ‘empirical interpolation’ method: application to efficient reduced-basis discretization of partial differential equations. *C. R. Math. Acad. Sci. Paris* **339** (2004) 667–672.
- [3] R. Becker and R. Rannacher, An optimal control approach to a posteriori error estimation in finite element methods. *Acta Numer.* **10** (2001) 1–102.
- [4] L. Beirão da Veiga and M. Verani, A posteriori boundary control for FEM approximation of elliptic eigenvalue problems. *Numer. Methods Partial Differential Equations* **28** (2012) 369–388.
- [5] P. Binev, A. Cohen, W. Dahmen, R. DeVore, G. Petrova and P. Wojtaszczyk, Convergence rates for greedy algorithms in reduced basis methods. *SIAM J. Math. Anal.* **43** (2011) 1457–1472.
- [6] A. Buffa, Y. Maday, A.T. Patera, C. Prud’homme and G. Turinici, *A priori* convergence of the greedy algorithm for the parametrized reduced basis method. *ESAIM: M2AN* **46** (2012) 595–603.
- [7] E. Cancès, V. Ehrlacher and T. Lelièvre, Greedy algorithms for high-dimensional eigenvalue problems. *Constructive Approximation* **40** (2013) 387–423.
- [8] A. Cohen and R. DeVore, Approximation of high-dimensional parametric PDEs. *Acta Numerica*, 1–159 (2015).
- [9] L. Dedè, Reduced basis method and a posteriori error estimation for parametrized linear-quadratic optimal control problems. *SIAM J. Sci. Comput.* **32** (2010) 997–1019.
- [10] T. Dickopf, T. Horgan and B. Wohlmuth, Simultaneous reduced basis approximation of parameterized eigenvalue problems. Preprint [arXiv:1506.09200](https://arxiv.org/abs/1506.09200) (2015).
- [11] D.C. Dobson and F. Santosa, Optimal localization of eigenfunctions in an inhomogeneous medium. *SIAM J. Appl. Math.* **64** (2004) 762–774.
- [12] L. Evans, Partial differential equations. Vol. 19 of *Graduate Studies in Mathematics*, 2nd edition. American Mathematical Society, Providence, RI (2010).
- [13] M. Fares, J. Hesthaven, Y. Maday and B. Stamm, The reduced basis method for the electric field integral equation. *J. Comp. Phys.* **230** (2011) 5532–5555.
- [14] G.H. Golub and C.F. Van Loan, *Matrix Computations*, 4th edition. The John Hopkins University Press, Baltimore (2013).
- [15] J.S. Hesthaven, G. Rozza and B. Stamm, Certified Reduced Basis Methods for Parametrized Partial Differential Equations. *Springer Briefs in Mathematics*. Springer (2016).
- [16] V. Heuveline and R. Rannacher, A posteriori error control for finite approximations of elliptic eigenvalue problems. *Adv. Comput. Math.* **15** (2001) 107–138.
- [17] M. Hintermüller, C.-Y. Kao and A. Laurain, Principal eigenvalue minimization for an elliptic problem with indefinite weight and Robin boundary conditions. *Appl. Math. Optim.* **65** (2012) 111–146.
- [18] D.B.P. Huynh, D.J. Knezevic and A.T. Patera. A static condensation reduced basis element method: approximation and a posteriori error estimation. *ESAIM: M2AN* **47** (2013) 213–251.
- [19] T. Lassila and G. Rozza, Parametric free-form shape design with PDE models and reduced basis method. *Comput. Meth. Appl. Mech. Engrg.* **199** (2010) 1583–1592.
- [20] T. Lassila, A. Manzoni, A. Quarteroni and G. Rozza, Model order reduction in fluid dynamics: challenges and perspectives. In *Reduced order methods for modeling and computational reduction*, edited by A. Quarteroni and G. Rozza. Vol. 9. *Springer, MS&A Series* (2013) 235–274.
- [21] L. Machiels, Y. Maday, I. Oliveira, A.T. Patera and D. Rovas, Output bounds for reduced-basis approximations of symmetric positive definite eigenvalue problems. *C. R. Acad. Sci. Paris Sér. I Math.* **331** (2000) 153–158.
- [22] Y. Maday, A.T. Patera and J. Peraire, A general formulation for a posteriori bounds for output functionals of partial differential equations; application to the eigenvalue problem. *C. R. Acad. Sci. Paris, Série I* **327** (1998) 823–828.
- [23] A. Manzoni, An efficient computational framework for reduced basis approximation and a posteriori error estimation of parametrized Navier–Stokes flows. *ESAIM: M2AN* **48** (2014) 1199–1226.
- [24] A. Manzoni, A. Quarteroni and G. Rozza, Shape optimization of cardiovascular geometries by reduced basis methods and free-form deformation techniques. *Int. J. Numer. Meth. Fluids* **70** (2012) 646–670.
- [25] A. Manzoni and F. Negri, Heuristic strategies for the approximation of stability factors in quadratically nonlinear parametrized PDEs. *Adv. Comput. Math.* **41** (2015) 1255–1288.
- [26] J.A. Méndez-Bermúdez and F.M. Izrailev, Transverse localization in quasi-1d corrugated waveguides (2008) 1376–1378.
- [27] J. Nečas, *Les méthodes directes en théorie des équations elliptiques*. Masson et Cie, Paris; Academia, Prague (1967).
- [28] F. Negri, G. Rozza, A. Manzoni and A. Quarteroni, Reduced basis method for parametrized elliptic optimal control problems. *SIAM J. Sci. Comput.* **35** (2013) A2316–A2340.
- [29] N.C. Nguyen, K. Veroy and A.T. Patera, Certified real-time solution of parametrized partial differential equations. In *Handbook of Materials Modeling*, edited by S. Yip (2005) 1523–1558.
- [30] S.J. Osher and F. Santosa, Level set methods for optimization problems involving geometry and constraints i. frequencies of a two-density inhomogeneous drum. *J. Comput. Phys.* **171** (2001) 272–288.

- [31] G.S.H. Pau, *Reduced Basis Method for Quantum Models of Crystalline Solids*. Ph.D. thesis, Massachusetts Institute of Technology (2007).
- [32] C. Prud'homme, D. Rovas, K. Veroy, Y. Maday, A.T. Patera and G. Turinici, Reliable real-time solution of parametrized partial differential equations: reduced-basis output bounds methods. *J. Fluids. Engng.* **124** (2002) 70–80.
- [33] A. Quarteroni, G. Rozza and A. Manzoni, Certified reduced basis approximation for parametrized partial differential equations in industrial applications. *J. Math. Ind.* **1** (2011).
- [34] A. Quarteroni, A. Manzoni and F. Negri, *Reduced Basis Methods for Partial Differential Equations. An Introduction*. Vol. 92 of *Unitext Series*. Springer (2016).
- [35] D.V. Rovas, *Reduced-Basis Output Bound Methods for Parametrized Partial Differential Equations*. Ph.D. thesis, Massachusetts Institute of Technology (2003).
- [36] G. Rozza, D.B.P. Huynh and A. Manzoni, Reduced basis approximation and a posteriori error estimation for Stokes flows in parametrized geometries: roles of the inf-sup stability constants. *Numer. Math.* **125** (2013) 115–152.
- [37] B. Sapoval, O. Haeberlé and S. Russ, Acoustical properties of irregular and fractal cavities. *Acoust. Soc. Am. J.* **102** (1997) 2014–2019.